Edinburgh Research Explorer

Spatiotemporal variability of dissolved inorganic macronutrients along the northern Antarctic Peninsula (1996–2019)

LIMNOLOGY and OCEANOGRAPHY

Spatiotemporal variability of dissolved inorganic macronutrients along the northern Antarctic Peninsula (1996–2019)

Thiago Monteiro [1,2,3,4]* **Sian F. Henley,** [4] **Ricardo César Gonçalves Pollery,** [5]
Carlos Rafael Borges Mendes [2,6] **Mauricio Mata** [1,2] **Virginia Maria Tavano** [6]
Carlos Alberto Eiras Garcia, [1,2] **Rodrigo Kerr** [1,2,3]*

[1]Programa de Pós-Graduação em Oceanologia, Instituto de Oceanografia, Universidade Federal do Rio Grande (FURG), Rio Grande, Brazil
[2]Laboratório de Estudos dos Oceanos e Clima, Instituto de Oceanografia, Universidade Federal do Rio Grande (FURG), Rio Grande, Brazil
[3]Brazilian Ocean Acidification Network (BrOA), Rio Grande, Brazil
[4]School of GeoSciences, University of Edinburgh, Edinburgh, UK
[5]Unidade Multiusuário de Análises Ambientais, Centro de Ciências da Saúde, Universidade Federal do Rio de Janeiro (UFRJ), Cidade Universitária, Rio de Janeiro, Brazil
[6]Laboratório de Fitoplâncton e Micro-organismos Marinhos, Instituto de Oceanografia, Universidade Federal do Rio Grande (FURG), Rio Grande, Brazil

Abstract

The northern Antarctic Peninsula is a key region of the Southern Ocean due to its complex ocean dynamics, distinct water mass sources, and the climate-driven changes taking place in the region. Despite the importance of macronutrients in supporting strong biological carbon uptake and storage, little is known about their spatiotemporal variability along the northern Antarctic Peninsula. Hence, we explored for the first time a 24-year time series (1996–2019) in this region to understand the processes involved in the spatial and interannual variability of macronutrients. We found high macronutrient concentrations, even in surface waters and during strong phytoplankton blooms. Minimum concentrations of dissolved inorganic nitrogen (DIN; 16 μmol kg^{-1}), phosphate (0.7 μmol kg^{-1}), and silicic acid (40 μmol kg^{-1}) in surface waters are higher than those recorded in surrounding regions. The main source of macronutrients is the intrusions of Circumpolar Deep Water and its modified variety, while local sources (organic matter remineralization, water mass mixing, and mesoscale structures) can enhance their spatiotemporal variability. However, we identified a depletion in silicic acid due to the influence of Dense Shelf Water from the Weddell Sea. Macronutrient concentrations show substantial interannual variability driven by the balance between the intrusions of modified Circumpolar Deep Water and advection of Dense Shelf Water, which is largely modulated by the Southern Annular Mode (SAM) and to some extent by El Niño-Southern Oscillation (ENSO). These findings are critical to improving our understanding of the natural variability of this Southern Ocean ecosystem and how it is responding to climate changes.

*Correspondence: thiagomonteiro@furg.br; rodrigokerr@furg.br

Additional Supporting Information may be found in the online version of this article.

The Southern Ocean plays a critical role in regulating the global climate (Henley et al. 2020). Although Southern Ocean surface waters cover less than 20% of the global ocean, they account for 40–50% of the total oceanic uptake of anthropogenic carbon from the atmosphere (Keppler and Landschützer 2019). Part of the carbon uptake in the Southern Ocean is driven by photosynthesis during the summer, which is fueled by high concentrations of macronutrients, supporting ecosystem functioning and carbon storage (Henley et al. 2020). Nevertheless, the Southern Ocean is one of the regions that experiences pronounced changes in biogeochemical properties, altering the functioning of the entire ecosystem (Henley et al. 2020 and references therein). A key region for understanding biogeochemical changes in the Southern Ocean is the northern Antarctic Peninsula, which has experienced rapid changes in the coupled atmosphere–ocean–cryosphere system (Kerr et al. 2018a; Henley et al. 2019). For example, investigations over the last two decades have reported changes in wind patterns, land and sea ice cover, biological activity, and the carbonate system (Kerr et al. 2018c; Henley et al. 2019).

The micronutrient iron is an important fuel for photosynthesis and is known to be limiting for primary production in vast areas of the Southern Ocean (de Baar et al. 1995; Henley et al. 2020). However, the regions around the northern Antarctic Peninsula were shown to have sufficient iron supply to sustain high levels of phytoplankton production and biomass (Ardelan et al. 2010). Moreover, the northern Antarctic Peninsula is important within the Southern Ocean because it has one of the coastal regions most impacted by the Antarctic Circumpolar Current, which carries the Circumpolar Deep Water. Circumpolar Deep Water is a relatively old water mass mainly sourced from mixing along the Antarctic Circumpolar Current between the North Atlantic Deep Water and deep waters from Indian and South Pacific Oceans (Ferreira and Kerr 2017), so it is low in dissolved oxygen and rich in remineralized carbon and macronutrients (Prézelin et al. 2000; Hauri et al. 2015). Hence, the northern Antarctic Peninsula is constantly influenced by Circumpolar Deep Water intrusions (Barlett et al. 2018; Wang et al. 2022), altering the biogeochemical dynamics in this region (Henley et al. 2019; Orselli et al. 2022; Santos-Andrade et al. 2023). The Circumpolar Deep Water is a relatively warm water mass (> 1°C) that intrudes into the intermediate layers along the northern Antarctic Peninsula (Prézelin et al. 2000; Venables et al. 2017). The physical properties of Circumpolar Deep Water change as it is mixed with cooler and less saline waters, forming the modified Circumpolar Deep Water in the shelf and coastal domain (Venables et al. 2017; Wang et al. 2022).

The northern Antarctic Peninsula coastal region encompasses the Gerlache and Bransfield Straits, and the northwestern Weddell Sea continental shelf (Fig. 1). At the southernmost part of the northern Antarctic Peninsula, the Gerlache Strait is a relatively shallow region (depth $\sim$ 800 m), with high concentrations of sea ice (Parra et al. 2020; Monteiro et al. 2020a) and

strongly impacted by meltwater from continental glaciers (Meredith et al. 2022). Despite covering a small area, Gerlache Strait acts as a stronger summer CO_2 sink than larger regions such as Bransfield Strait (Monteiro et al. 2020b). This strong CO_2 sink behavior is driven mainly by high primary productivity (Costa et al. 2020; Monteiro et al. 2020b), which sustains a diverse and productive food web (Anadón and Estrada 2002; Kerr et al. 2018a). Indeed, intense blooms of diatoms (Costa et al. 2020) and high densities of krill, penguins, and whales are recorded in Gerlache Strait (Anadón and Estrada 2002; Kerr et al. 2018a). Toward the north, the Bransfield Strait is a region with rapid and dynamic ocean circulation (Zhou et al. 2002; Sangrà et al. 2017) and comprises the western, central, and eastern basins, separated by relatively shallow sills (Fig. 1b). The western basin is the shallowest ($\sim$ 1000 m), followed by the central ($\sim$ 2000 m) and eastern ($\sim$ 2500 m) basins.

The northern Antarctic Peninsula surface circulation (Fig. 1a) is characterized by local surface water and the modified Circumpolar Deep Water at upper levels, mainly coming from the Bellingshausen Sea (Zhou et al. 2002; Sangrà et al. 2017). These surface waters are advected from the Gerlache Strait to the eastern basin of Bransfield Strait by the Bransfield Current (Zhou et al. 2002; Moffat and Meredith 2018). This current flows in a southwest-to-northeast direction along the shelf break of the South Shetland Islands (Sangrà et al. 2017). The waters advected by the Bransfield Current are relatively warm ($\sim$ 1.25°C) and highly productive (Mendes et al. 2018; Costa et al. 2020, 2021), being able to transport significant biomass of phytoplankton and zooplankton along the northern Antarctic Peninsula (Ferreira et al. 2020). The western basin of Bransfield Strait is strongly influenced by modified Circumpolar Deep Water intrusions at intermediate levels (Barlett et al. 2018; Wang et al. 2022), while the central and eastern deep basins are fueled by Dense Shelf Water from the Weddell Sea (Dotto et al. 2016; Damini et al. 2022). Dense Shelf Water refers to distinct shelf water varieties (i.e., High-Salinity Shelf Water and Low-Salinity Shelf Water; Damini et al. 2022; Wang et al. 2022) sourced in the northwestern continental shelf region of the Weddell Sea (Van Caspel et al. 2018; Wang et al. 2022), east of the Antarctic Peninsula (Fig. 1). Unlike modified Circumpolar Deep Water, Dense Shelf Water is recently ventilated under the shelf domain, therefore it is cold ($< -1°C$) and rich in dissolved oxygen (Dotto et al. 2016; Damini et al. 2022).

The Dense Shelf Water is advected into the northern Antarctic Peninsula and retained with its most pure form mainly in the deep layer of the central basin of Bransfield Strait (Dotto et al. 2016), while an intense mixing changing its physical (Damini et al. 2022; Wang et al. 2022) and biogeochemical (Santos-Andrade et al. 2023) properties occurs with modified Circumpolar Deep Water at upper levels. Hence, while modified Circumpolar Deep Water is transported from the south at intermediate layers along the northern Antarctic Peninsula, the Dense Shelf Water is advected in deeper layers
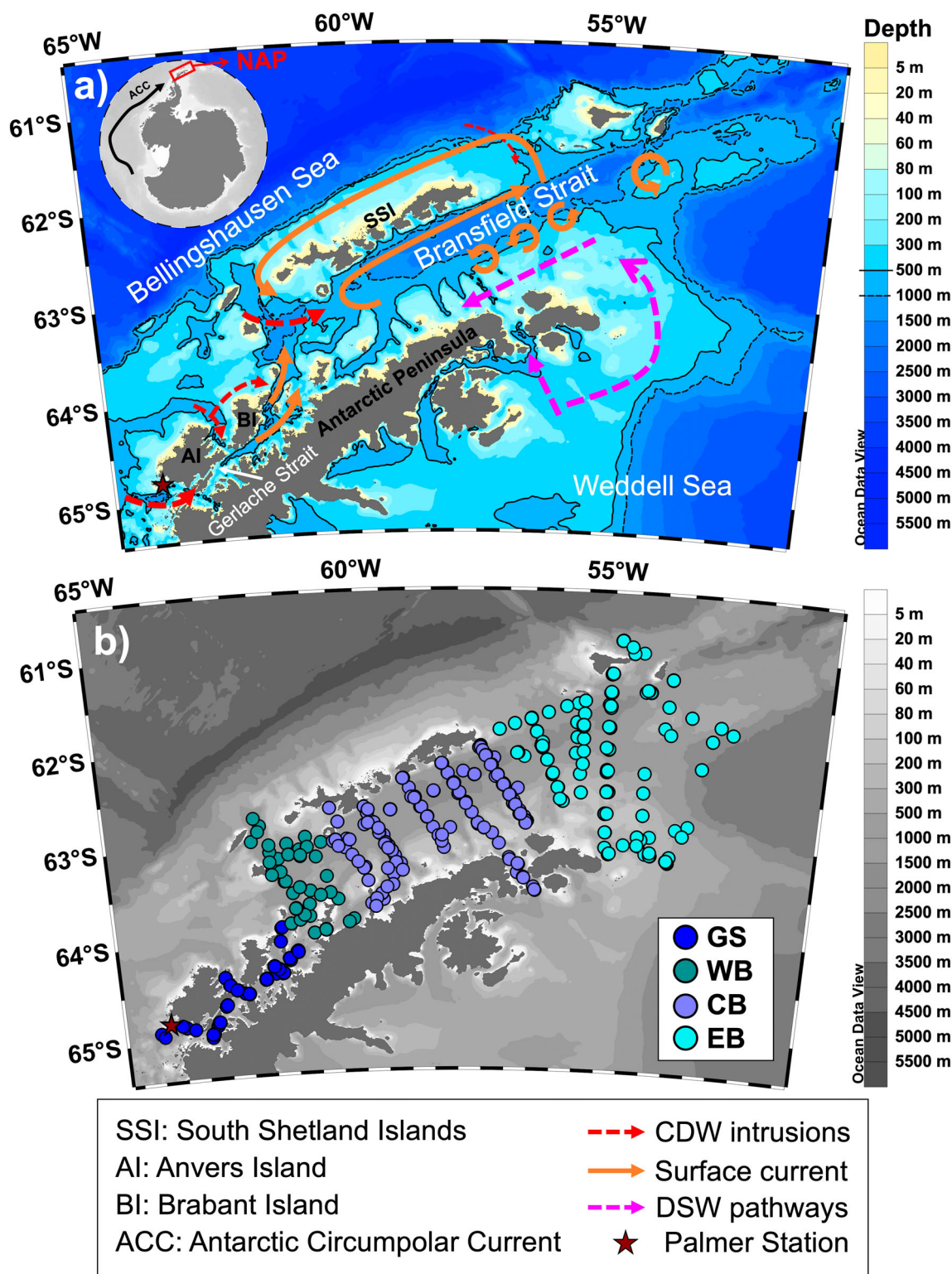
Fig. 1. Maps of the northern Antarctic Peninsula (NAP) region showing (**a**) geographic features and ocean circulation patterns, and (**b**) sampling stations examined in this study. In (**a**), the surface circulation (orange arrows), regions of mesoscale structures, as well as Circumpolar Deep Water (CDW) and Dense Shelf Water (DSW) pathways were based on previous studies (Sangrà et al. 2017; Moffat and Meredith 2018; Wang et al. 2022). The brown star in (**a**) and (**b**) depicts the U.S. Palmer Station location (64.8°S, 64.1°W), from which we extracted dissolved oxygen data (Waite 2022) used in Fig. 9 and macronutrient data (Ducklow et al. 2019) to validate the seasonal drawdown approach described in the methods. In (**b**), the distribution of hydrographic stations where macronutrients were sampled include: Gerlache Strait (GS; dark blue dots), western (WB, green dots), central (CB, purple dots), and eastern (EB, cyan dots) basins of the Bransfield Strait.

from the north (Moffat and Meredith 2018; Wang et al. 2022). On interannual timescales, the strength of modified Circumpolar Deep Water intrusion and Dense Shelf Water advection along the northern Antarctic Peninsula is driven by regional modes of climate variability, such as the Southern Annular Mode (SAM) and the El Niño–Southern Oscillation (ENSO) (Barlett et al. 2018; Damini et al. 2022). During positive SAM and/or negative ENSO, modified Circumpolar Deep Water intrusion is intensified, weakening the spreading of Dense Shelf Water along the northern Antarctic Peninsula. Conversely, when SAM is negative and/or ENSO is positive, Dense Shelf Water advection is strengthened and can reach the Gerlache Strait (Wang et al. 2022). Indeed, the Dense Shelf Water in the Gerlache Strait has already been identified through thermohaline signals (Parra et al. 2020; Wang et al. 2022) and anthropogenic carbon concentrations (Lencina-Avila et al. 2018; Kerr et al. 2018*b*).

Furthermore, the environments along the northern Antarctic Peninsula are influenced by mesoscale oceanographic processes that add complexity to the understanding of biogeochemistry in this region. The effect of shallow topography facilitates the upwelling of modified Circumpolar Deep Water in Gerlache Strait and the western basin of Bransfield Strait (Venables et al. 2017; Parra et al. 2020). However, little is known about its influence on the variability of macronutrient concentrations along the northern Antarctic Peninsula (Henley et al. 2019). The effect of topography and ocean circulation also leads to the formation of mesoscale eddies and increased eddy-fueled productivity in the eastern basin of Bransfield Strait (Wang et al. 2022; Damini et al. 2023), although these processes are often neglected in biogeochemical studies due to their complexity. Understanding temporal variability patterns of macronutrients is also a challenge along the northern Antarctic Peninsula, because the response time to SAM and ENSO variability modes is not well elucidated (Barlett et al. 2018; Wang et al. 2022) and the mesoscale processes themselves may also play an important role in this variability (Kerr et al. 2018*a*; Henley et al. 2019). For example, intense diatom blooms enhance CO_2 uptake (Anadón and Estrada 2002; Costa et al. 2020) and can lead to nutrient depletion in the upper ocean and subsequently increase the local remineralization of carbon and macronutrients below the mixed layer (Henley et al. 2017, 2018). In addition, melting sea ice and glacial ice regulates summer water column stability (Wang et al. 2020; Meredith et al. 2022), driving phytoplankton blooms (Kim et al. 2016; Costa et al. 2020), CO_2 uptake (Costa et al. 2020; Monteiro et al. 2020*b*), and nutrient depletion and replenishment in the upper ocean (Henley et al. 2017, 2018).

The importance of nutrients to fuel the primary production that underpins the food web has been emphasized in some studies throughout the northern Antarctic Peninsula (Anadón and Estrada 2002; Henley et al. 2019), as well as the impact of mesoscale processes on nutrient supply (Forsch et al. 2021;

Meredith et al. 2022). Furthermore, some studies have shown that macronutrient concentrations south of the northern Antarctic Peninsula, at Marguerite and Ryder Bays, are mainly regulated by Circumpolar Deep Water intrusions (Henley et al. 2017, 2018; Jones et al. 2023), nutrient regeneration and local features such as deep glacially scoured canyons (Henley et al. 2019 and references therein). Nevertheless, little is known about what regulates the spatial and temporal variability of macronutrient distributions due to the high complexity and heterogeneity biogeochemical provinces along the northern Antarctic Peninsula. We address these knowledge gaps by exploring a novel data set comprising 24 years (1996–2019) of macronutrient and hydrographic data to understand the oceanographic and biogeochemical processes involved in the spatial and temporal variability of macronutrients during the austral summer along the northern Antarctic Peninsula. Moreover, we examine the influence of the SAM and ENSO events on macronutrient inventories in this region.

Materials and methods

The hydrographic and macronutrient data sets

We compiled a time series spanning the period from 1996 to 2019 (Supporting Information Figs. S1–S4) of the seawater hydrographic variables conservative temperature (°C), absolute salinity (g kg^{-1}) and dissolved oxygen (μmol kg^{-1}), and the macronutrient concentrations nitrate, nitrite, ammonium, phosphate, and silicic acid (μmol kg^{-1}). The study area covered the northern Antarctic Peninsula regions including the Gerlache Strait, which separates the Anvers and Brabant Islands from the Antarctic Peninsula, and the Bransfield Strait, between the South Shetland Islands and the Peninsula (Fig. 1a). To better understand the different processes influencing the variability of macronutrient concentrations, the sampling stations were split into four subregions: the Gerlache Strait and the western, central, and eastern basins of Bransfield Strait (Fig. 1b). Most data ($\sim$ 90%) were obtained from the Brazilian High Latitude Oceanography Group (GOAL; Mata et al. 2018; Dotto et al. 2021) from austral summer field campaigns (January–March). In some years (1996, 2005, 2006, 2010, 2011), we used hydrographic and macronutrient data from GLODAPv2.2020 (Olsen et al. 2020) along the northern Antarctic Peninsula and exceptionally for 1996 we used data available from December 1995 to February 1996 (the FRUELA cruises, Anadón and Estrada 2002). Macronutrient concentrations from GLODAPv2.2020 were determined by colorimetric methods using the gas segmented continuous flow autoanalyzer (Hoppema et al. 2015). Details on the sampling and analysis of macronutrient data obtained from GLODAPv2.2020 data set can be found in the references shown in Supporting Information Table S1. The overall precision for most of these data was better than 0.95% for DIN, 1.09% for phosphate, and 1.28% for silicic acid (Hoppema et al. 2015).

Sampling and macronutrient analyses from GOAL data set

For the GOAL data set, hydrographic data profiles were measured, and discrete seawater samples were collected using a combined Sea-Bird CTD/Carousel 911 + system® equipped with oxygen sensors and Niskin bottles. Seawater samples were filtered through cellulose acetate membrane filters (0.45 μm) for determination of dissolved inorganic macronutrient concentrations (i.e., DIN: nitrate, nitrite, and ammonium; phosphate and silicic acid). Prior to 2015 (except 2003–2005), the analyses were carried out on board immediately after collection and from 2015 onwards the samples were frozen immediately at $-20°C$ until laboratory analysis. In both cases, the analyses followed the spectrophotometric determination methods described by Aminot and Chaussepied (1983) with an overall accuracy better than $\pm 3\%$ for DIN and phosphate and $\pm 5\%$ for silicic acid throughout the data set. Silicic acid measurements, in the form of reactive Si, were corrected for sea salt interference. Detection limits were 0.11 μmol kg^{-1} for DIN, 0.10 μmol kg^{-1} for phosphate, and 0.50 μmol kg^{-1} for silicic acid. Different instruments have been used over the years with common standards for DIN (ISO 13395), phosphate (ISO 15681-1), and silicic acid (ISO/FDIS 16264; Supporting Information Table S1). The reproducibility of the analyses, based on duplicates of the samples, was 1.0% for DIN, 0.7% for phosphate, and 1.0% for silicic acid, values very close to the macronutrient precisions estimated for GLODAPv2.2020 data. No certified nutrient reference material was used across the time series in either the GOAL or GLODAP databases, in common with other time series conducted over a comparable period (Hoppema et al. 2015; Kim et al. 2016).

Summer average profiles of hydrographic properties and macronutrients

About 97% of the DIN concentrations were composed of nitrate, followed by ammonium (2%) and nitrite (1%). In 1996, 2006, and 2011, we considered DIN as the concentration of nitrate and nitrite because no ammonium data were available, so the DIN concentration in these years may be underestimated by up to 2%. Discrete seawater samples were collected at regular depth intervals from surface (5 m) to deep waters (at approximately 15–5 m from the bottom). We averaged the parameters for each region at regular depth intervals from the surface to the bottom (i.e., 0, 25, 50, 75, 100, 250, 500, 750, 1000, 1250, 1500, and 2000 m) to obtain an averaged summer profile for each year (Supporting Information Figs. S1–S4). Then, all available data between 0 and 25 m were averaged to represent the depth level of 0 m; similarly, all available data between 25 and 50 m were averaged to represent the depth level of 25 m and so on. The macronutrient data density distribution for each depth level is shown in Supporting Information Fig. S5. All hydrographic and macronutrient data are available at BGQNAPv1.0: a summer macronutrients binned data set for the Northern Antarctic

Peninsula, Southern Ocean—https://doi.org/10.5281/zenodo.7384423 (Monteiro et al. 2022).

Seasonal macronutrient drawdown

We estimated seasonal macronutrient drawdown for the averaged profiles for each year (gray profiles in Fig. 5) as the difference between the depth-integrated nutrient concentration between 50 and 100 m and the depth-integrated concentration between 0 and 50 m as follows:

$$\text{Nutrient drawdown} = \int_{50\,m}^{100\,m}[\text{nutrients}]\,dz - \int_{0\,m}^{50\,m}[\text{nutrients}]\,dz$$

where [nutrients] refers to each macronutrient concentration in μmol kg^{-1}, that is, DIN, phosphate, or silicic acid.

Therefore, we assumed that summer macronutrient concentrations below the upper mixed layer depth (below 50 m) were representative of macronutrient concentrations at the sea surface (above 50 m) in the previous winter, as has been shown in other studies in adjacent regions (Henley et al. 2018). Although the upper mixed layer depth is expected to vary both spatially and temporally, the choice of the 50-m threshold is consistent with in situ measurements over the long time series at Palmer Station (Kim et al. 2016) and spatially along the northern Antarctic Peninsula (Costa et al. 2020, 2023). Moreover, the range ($-1.96°C$ to $1.10°C$) and average ($-0.74 \pm 0.44°C$) of minimum temperature between 50 and 100 m in summer are in reasonable agreement with the range ($-1.97°C$ to $-0.76°C$) and average ($-1.54 \pm 0.23°C$) of minimum temperature between 0 and 50 m in winter from the northern Antarctic Peninsula seasonal hydrographic climatology (Dotto et al. 2021). This suggests that the remnant Winter Water layer persists in summer at ~ 50 to 100 m, as has been observed in other hydrographic studies along the northern Antarctic Peninsula (Wang et al. 2022). This approach was also applied to estimate the seasonal macronutrient drawdown for the averaged profiles for each year in the Palmer Station LTER data (Fig. 1; Ducklow et al. 2019), where Kim et al. (2016) measured seasonal macronutrient drawdown from in situ data collected in winter and the following summer in the upper 50 m. Our estimates of seasonal macronutrient drawdown agree well with the results obtained by Kim et al. (2016), which attests to the robustness of the adopted method based on summer data alone. They measured a seasonal drawdown in the upper 50 m from 1993 to 2013 of 415 ± 110, 23 ± 10, and 985 ± 386 mmol m^{-2} for DIN, phosphate, and silicic acid, respectively. For the same period, we estimated a seasonal drawdown of 411 ± 191, 25 ± 9, and 950 ± 269 mmol m^{-2} for DIN, phosphate, and silicic acid, respectively.

Composite macronutrient profiles by climate modes

To assess the influence of the SAM on the concentrations of macronutrients, we separated the austral summer

profiles between years of positive SAM (SAM+) and negative SAM (SAM−) indexes. We computed an average profile for each set of years (or SAM events), and then calculated the difference between the averages (i.e., Δnutrient) as follows:

$$\Delta \text{nutrient} = \overline{[\text{nutrient}]}_{\text{SAM+}} - \overline{[\text{nutrient}]}_{\text{SAM−}}$$

where the average terms under the bars are the averages of the nutrient concentrations (i.e., [nutrient] = DIN, phosphate, or silicic acid in μmol kg^{-1}) for the profiles in years of positive and negative SAM. Thus, positive (negative) values of Δ*nutrient* mean that there are higher (lower) macronutrient concentrations during positive SAM years and vice versa for negative SAM. The approach was also applied for ENSO events, that is, positive and negative ENSO events (*see* Supporting Information Table S2 for the years of each SAM and ENSO events).

Southern Annular Mode index was obtained from the British Antarctic Survey website (http://www.nerc-bas.ac.uk/icd/gjma/sam.html; accessed on 01 March 2021), which is based on the differences between normalized monthly zonal means of sea-level pressure observations at 40°S and 65°S (Marshall et al. 2006). ENSO index was obtained from the U.S. Climate Prediction Centre (http://www.cpc.ncep.noaa.gov; accessed on 01 March 2021), which is defined as the consecutive 3-month average of sea surface temperature anomalies from the ERSST.v4 data set in the Niño 3.4 region (5°N–5°S, 120°W–170°W; Vera and Osman 2018). Although the response time of physical and biogeochemical properties to variations in SAM and ENSO along the northern Antarctic Peninsula is not well understood, it has been estimated to range from 4 to 6 months for SAM and 6 to 9 months for ENSO (Kim et al. 2016; Barlett et al. 2018). Here, we used a lag of 4 months from the sampling month for the SAM index and 6 months for the ENSO index.

We calculated the uncertainty propagated in calculating the difference between the averages through the following equation:

$$\sigma_z = \sqrt{(\sigma_{\bar{x}})^2 + \left(\sigma_{\bar{y}}\right)^2}$$

where "$\sigma_{\bar{x}}$" and "$\sigma_{\bar{y}}$" are the standard errors of each average. To assess the statistical difference between the average profiles for positive and negative SAM or ENSO, we used Student's *t*-tests for normally distributed profiles. For profiles with non-normal distributions, we used the non-parametric Mann–Whitney–Wilcoxon test. To test the normal distribution, we used the Shapiro–Wilk statistical test.

Results

Spatial distribution of hydrographic properties and macronutrients along the northern Antarctic Peninsula

In general, the surface temperature was higher than 0°C along the northern Antarctic Peninsula (Fig. 2a). However, along the Bransfield Strait we observed waters colder than 0°C toward the Antarctic Peninsula and waters warmer than 0°C toward the South Shetland Islands (Supporting Information Fig. S7a–c). Throughout the water column, the temperature was higher than 0°C at Gerlache Strait, decreasing (< 0°C) along the Bransfield Strait (Fig. 2a). Temperatures higher than 0°C were observed at the southern end of Gerlache Strait and western basin of Bransfield Strait from the surface to the deep layer (Supporting Information Fig. S7). Temperatures lower than −1°C were observed in the central basin of Bransfield Strait below 500 m, while and a slight increase of temperature from −0.5 to 0.25°C was observed at the eastern end of Bransfield Strait below 500 m (Figure 2a). Salinity was lower above 50 m (34.28 ± 0.18 g kg^{-1}) along the northern Antarctic Peninsula (Fig. 2b), and even lower in Gerlache Strait (34.09 ± 0.25 g kg^{-1}; Supporting Information Fig. S7). Below 200 m the salinity was relatively homogeneous in the central basin of Bransfield Strait (34.70 ± 0.04 g kg^{-1}), while it was slightly higher in the western basin of Bransfield Strait (34.72 ± 0.02 g kg^{-1}) and in the Gerlache Strait (34.79 ± 0.05 g kg^{-1}; Fig. 2b). Dissolved oxygen concentrations were lowest (< 225 μmol kg^{-1}) below 50 m in the Gerlache Strait and western basin of Bransfield Strait, and highest (> 275 μmol kg^{-1}) in the central basin of Bransfield Strait, mainly below 1000 m (Fig. 2c).

The highest concentrations of DIN (> 35 μmol kg^{-1}) were observed in the transition between the central and eastern basins of Bransfield Strait below 500 m (Fig. 2d). Although the DIN concentrations did not have as clear a west–east pattern as the other macronutrients, in general a slightly higher DIN concentration was observed in the central basin of Bransfield Strait than other sub-regions. Average DIN concentration through the water column was 29.67 ± 3.09 μmol kg^{-1} in the Gerlache Strait and 28.23 ± 2.84, 30.39 ± 2.49, and 29.42 ± 2.08 μmol kg^{-1} in the western, central, and eastern basins of Bransfield Strait, respectively.

Both phosphate (Fig. 2e) and silicic acid (Fig. 2f) concentrations were higher in the Gerlache Strait and western basin of Bransfield Strait than the rest of the northern Antarctic Peninsula below the subsurface (50 m) down to 750 m. Average silicic acid concentration through the water column was 80.67 ± 8.99 μmol kg^{-1} in the Gerlache Strait and 74.71 ± 6.02, 60.93 ± 4.72, and 62.38 ± 7.87 μmol kg^{-1} in the western, central, and eastern basins of Bransfield Strait, respectively. Average phosphate concentration through the water column was 1.88 ± 0.26 μmol kg^{-1} in the Gerlache Strait and 2.00 ± 0.19, 1.86 ± 0.20, and
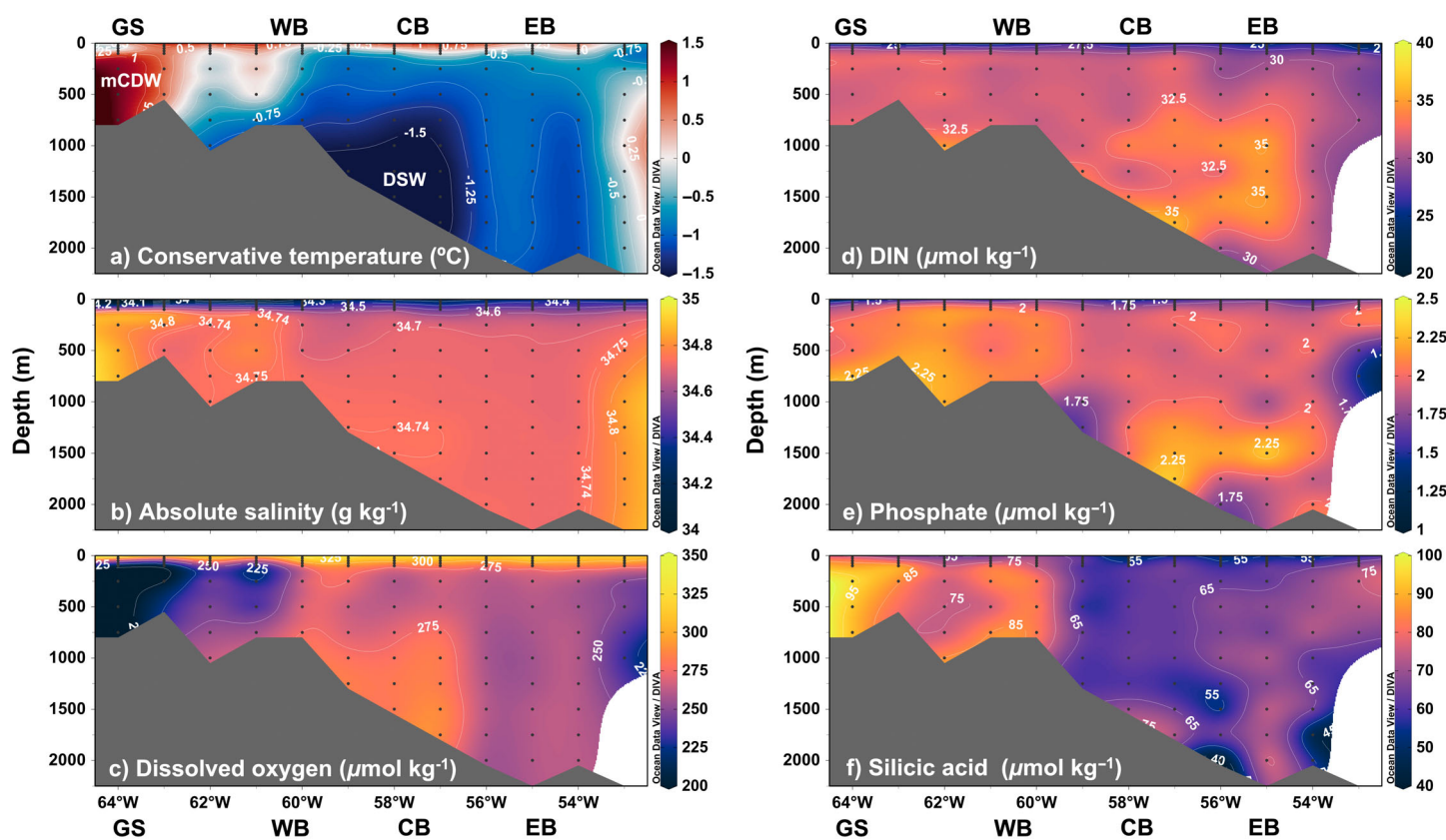
Fig. 2. Zonal sections of water column distributions of (**a**) conservative temperature, (**b**) absolute salinity, (**c**) dissolved oxygen, (**d**) DIN, (**e**) phosphate, and (**f**) silicic acid during austral summer (January to March) along the northern Antarctic Peninsula. Profiles composing each section are averaged profiles at each degree of longitude, considering the entire data set (from 1996 to 2019). The zonal section comprises the regions from the south to north of the northern Antarctic Peninsula: Gerlache Strait (GS), and the western (WB), central (CB), and eastern (EB) basins of Bransfield Strait. At the western end of the northern Antarctic Peninsula (GS), there are intense intrusions of modified Circumpolar Deep Water (mCDW) whereas in the EB and mainly CB there are intense intrusions of Dense Shelf Water (DSW) from the Weddell Sea. Sampling depths are shown as grey dots.

$1.88 \pm 0.17 \, \mu\text{mol kg}^{-1}$ in the western, central, and eastern basins of Bransfield Strait, respectively. We also observed high phosphate concentrations in both central $(2.00 \pm 0.21 \, \mu\text{mol kg}^{-1})$ and eastern $(1.99 \pm 0.15 \, \mu\text{mol kg}^{-1})$ basins of Bransfield Strait below 1000 m (Fig. 2e). In some profiles in the central and eastern basins of Bransfield Strait, there were concentrations of phosphate $(1.75 \, \mu\text{mol kg}^{-1})$ and silicic acid $(55 \, \mu\text{mol kg}^{-1})$ in the deep layer as low as in the surface layer (Fig. 2e,f). The lowest concentrations of silicic acid were recorded in the central basin of Bransfield Strait, from the surface to the deep layer (Supporting Information Fig. S7).

The distribution of hydrographic properties and macronutrients were associated with the modified Circumpolar Deep Water and Dense Shelf Water along the northern Antarctic Peninsula (Fig. 3). The lowest temperatures $(< -1^\circ\text{C})$ below 500 m were associated with a greater influence of Dense Shelf Water while the highest temperatures $(> 0^\circ\text{C})$ were associated with a greater influence of modified Circumpolar Deep Water in intermediate layers (Fig. 3a). Lower dissolved oxygen concentrations

$(< 225 \, \mu\text{mol kg}^{-1})$ were evident in warmer waters associated with the modified Circumpolar Deep Water in contrast to the more oxygenated $(> 275 \, \mu\text{mol kg}^{-1})$ waters associated with Dense Shelf Water (Fig. 3b). In general, the highest concentrations of phosphate $(> 2 \, \mu\text{mol kg}^{-1})$ and silicic acid $(> 80 \, \mu\text{mol kg}^{-1})$ were associated with greater influence of modified Circumpolar Deep Water (Fig. 3c–e) in intermediate and deep layers (Fig. 3a), although high concentrations of DIN $(> 30 \, \mu\text{mol kg}^{-1})$ and phosphate $(> 2 \, \mu\text{mol kg}^{-1})$ were observed under the influence of Dense Shelf Water (Fig. 3c,d). The lowest silicic acid concentrations below 500 m were observed under the influence of Dense Shelf Water, with concentrations $(< 60 \, \mu\text{mol kg}^{-1})$ as low as in the surface layer. However, silicic acid concentrations were also relatively high in the surface layer, reaching values $> 70 \, \mu\text{mol kg}^{-1}$ (Fig. 3c).

Interannual variability of hydrographic properties and macronutrients along the northern Antarctic Peninsula

The highest interannual variability in temperature was observed in the western basin of Bransfield Strait (Fig. 4d), also
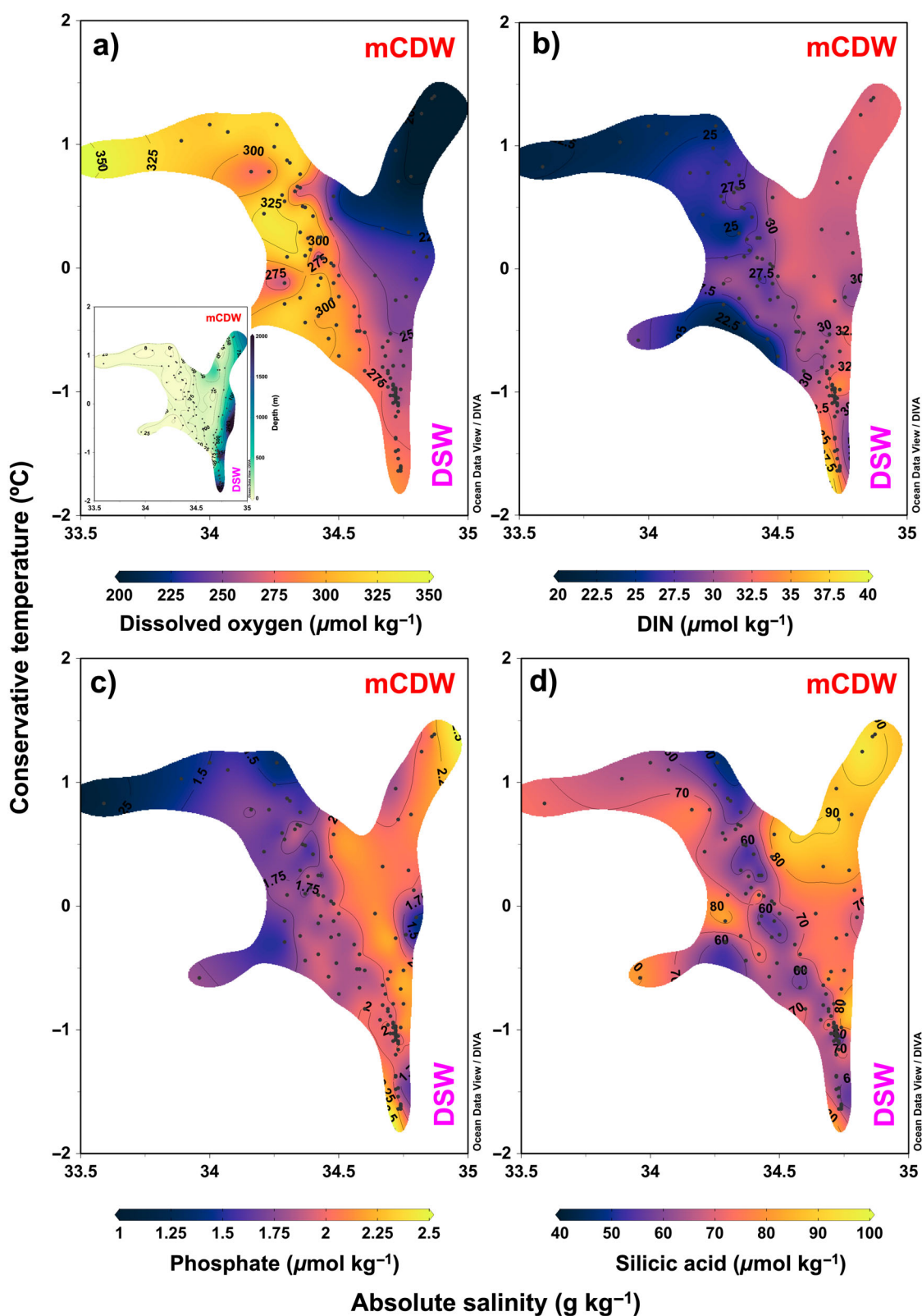
Fig. 3. Conservative temperature–absolute salinity ($\Theta - S_A$) plots showing biogeochemical properties with hydrographic properties during austral summer (January to March) along the northern Antarctic Peninsula. Shown are $\Theta - S_A$ vs. (**a**) dissolved oxygen, (**b**) DIN, (**c**) phosphate, (**d**) silicic acid, and depth on the inset (**a**). In each $\Theta - S_A$ diagram the influence of mixing of modified Circumpolar Deep Water (mCDW) and Dense Shelf Water (DSW) is shown.

Fig. 4. Summer (January–March) average profiles of hydrographic properties for each year from 1996 to 2019 along the northern Antarctic Peninsula, comprising the regions: (**a**–**c**) Gerlache Strait (GS), (**d**–**f**) western (WB), (**g**–**i**) central (CB), and (**j**–**l**) eastern (EB) basins of Bransfield Strait. Profiles for each year are presented in grey lines and the black lines are the averaged profiles over the period for each property and region. The horizontal black bars are the standard deviations for each depth. Years showing anomalous behavior (i.e., outside the standard deviation) are highlighted.
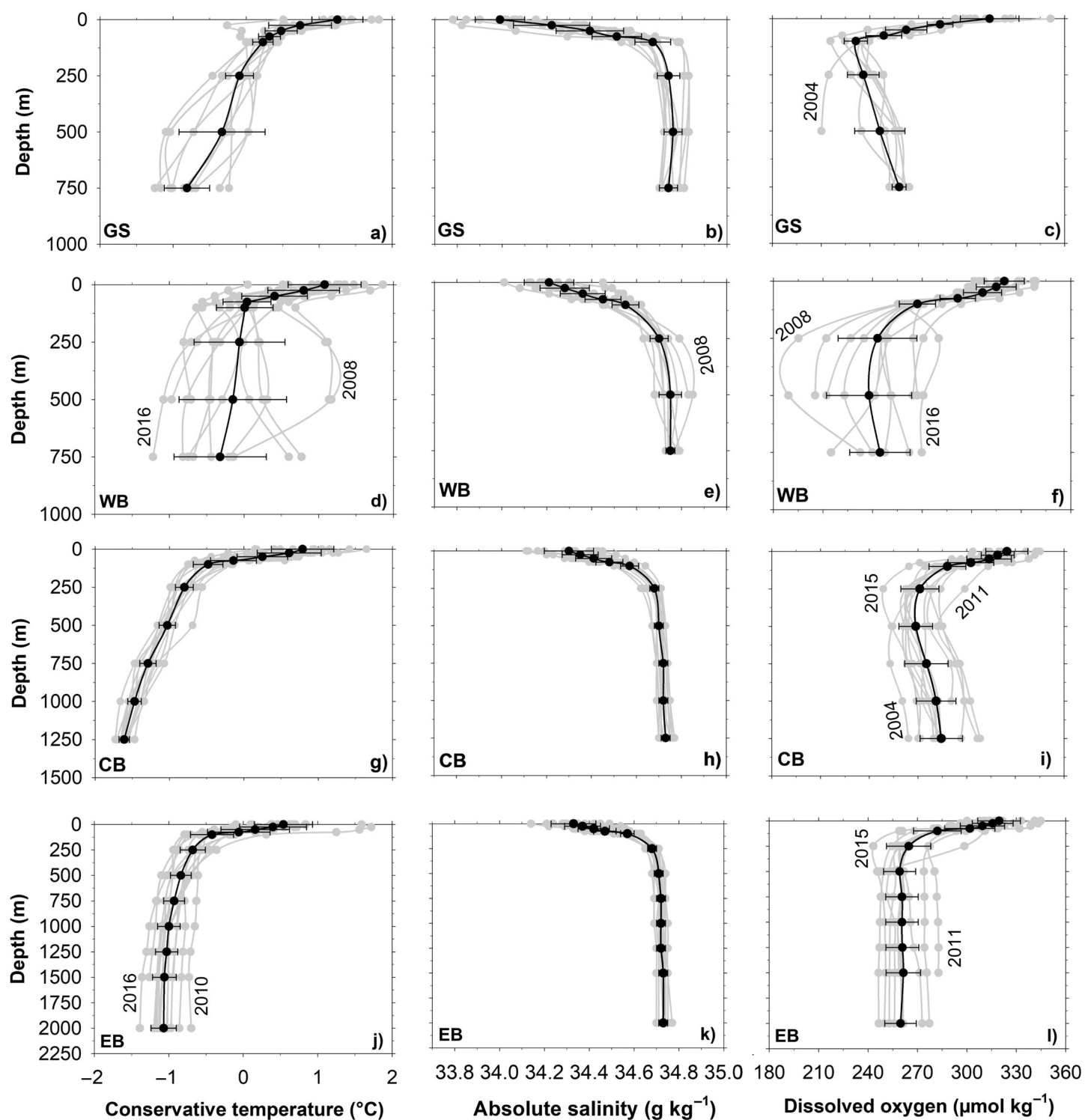
Fig. 5. Summer (January to March) averaged profiles of macronutrients for each year from 1996 to 2019 along the northern Antarctic Peninsula, comprising the regions: (**a–c**) Gerlache Strait (GS), and the (**d–f**) western (WB), (**g–i**) central (CB), and (**j–l**) eastern (EB) basins of Bransfield Strait. Profiles for each year are presented in grey lines and the black lines are the averaged profiles over the period for each property and region. The horizontal black bars are the standard deviations for each depth. Years showing anomalous behavior (i.e., outside the standard deviation) are highlighted.
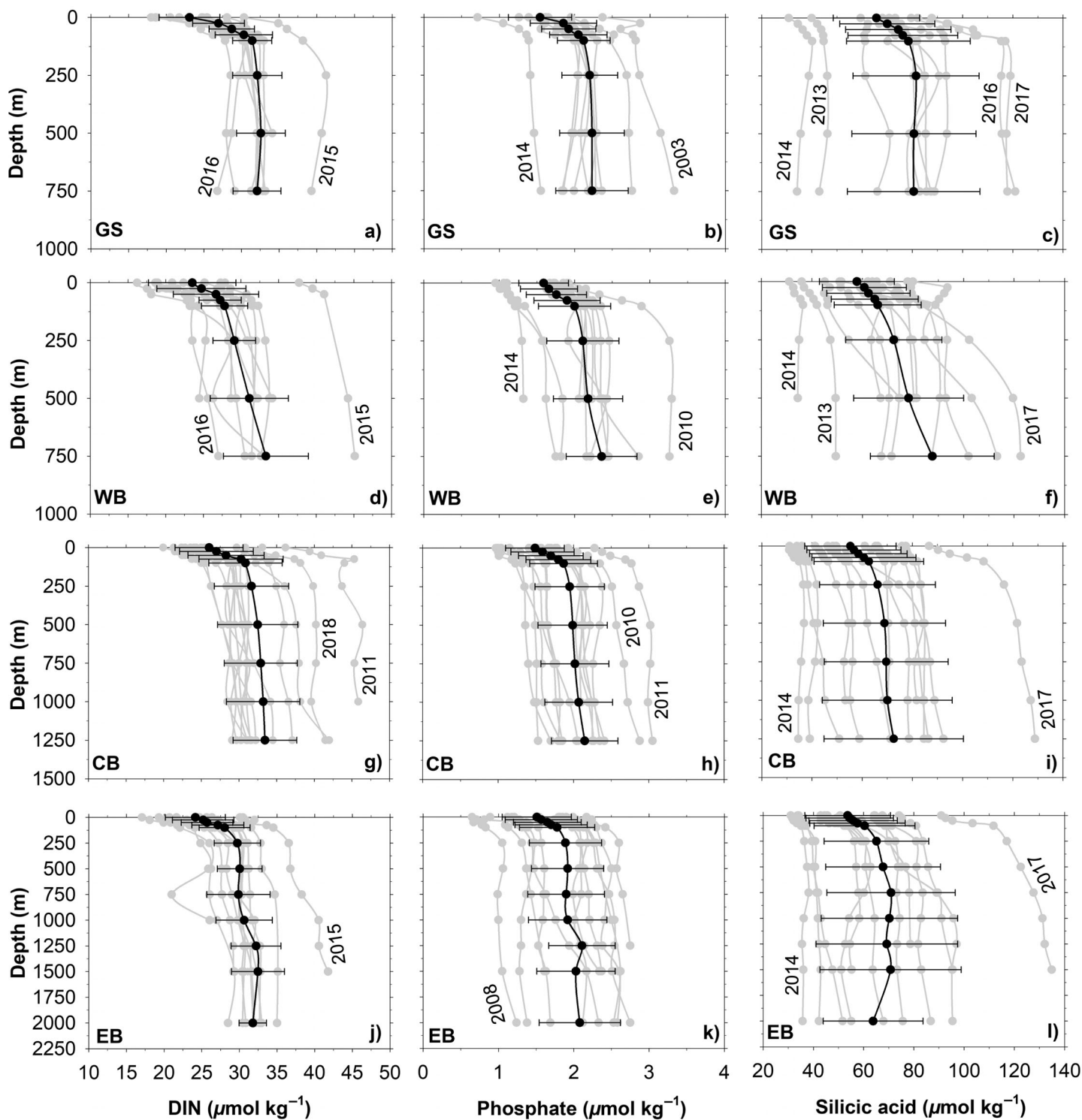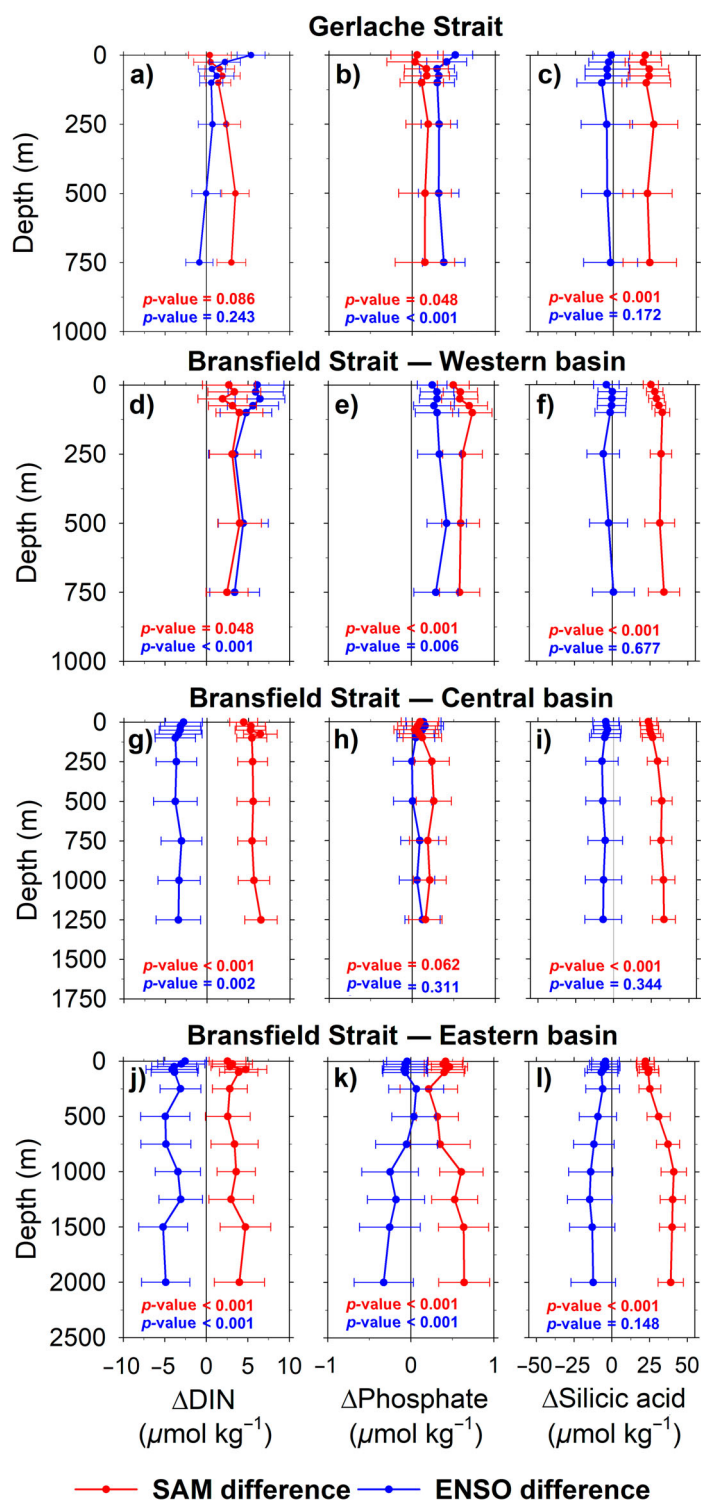
Fig. 6. Influence of Southern Annular Mode (SAM) and El Niño-Southern Oscillation (ENSO) modes of climate variability on the average profiles of macronutrients along the northern Antarctic Peninsula, comprising the regions: (**a**–**c**) Gerlache Strait and the (**d**–**f**) western, (**g**–**i**) central, and (**j**–**l**) eastern basins of Bransfield Strait. In red the difference in average profiles between positive and negative SAM (Δnutrient = DIN, phosphate, or silicic acid) is shown, while in blue the same is shown for ENSO. Positive (negative) values of Δnutrient mean that there are higher (lower)

associated with the highest variability of both salinity (Fig. 4e) and dissolved oxygen, mainly in the depth interval 250–500 m (Fig. 4f) in the same area. Dissolved oxygen concentrations also showed interannual variability in the central (Fig. 4i) and eastern (Fig. 4l) basins of Bransfield Strait, albeit to a lesser degree and more homogeneously with depth. In the western basin of Bransfield Strait, there was an increase of more than 1°C between 250 and 500 m with a subsequent decrease in the deep layer (Fig. 4d) in 2008, when the highest salinities (Fig. 4e) and the lowest concentrations of dissolved oxygen (Fig. 4f) were also observed. Conversely, in the western and eastern basins of Bransfield Strait the temperature was anomalously lower than −1°C below 500 m in 2016, when the highest concentrations of dissolved oxygen (> 270 μmol kg^{-1}) below 250 m in the western basin of Bransfield Strait were also observed (Fig. 4f). Gerlache Strait showed the second highest interannual variability in temperature and salinity among the regions examined here (Fig. 4b,c). Even in the eastern basin of Bransfield Strait, with less temperature variability, there were variations of up to 1°C among the years, but more homogeneously with depth (Fig. 4j) than in the western basin of Bransfield Strait and Gerlache Strait. Other anomalous behaviors were recorded, such as the lowest concentration of dissolved oxygen in 2004 in Gerlache Strait (Fig. 4c) and central basin of Bransfield Strait (Fig. 4i), and in 2015 in the central (Fig. 4i) and eastern (Fig. 4l) basins of Bransfield Strait at 250 m. On the other hand, anomalously high concentrations of dissolved oxygen in central (Fig. 4i) and eastern (Fig. 4l) basins of Bransfield Strait were recorded in 2011.

There was high interannual variability in the summer average profiles of all macronutrients along the northern Antarctic Peninsula (Fig. 5). The highest interannual variability was observed in silicic acid, with concentrations varying by up to a factor of three ($\sim$ 40–120 μmol kg^{-1}) through the water column (third column in Fig. 5). In most profiles, the concentration of silicic acid increased from surface waters to $\sim$ 100–200 m and then became more homogeneous with depth. DIN (first column in Fig. 5) and phosphate (second column in Fig. 5) concentrations were lower at the surface and consistently higher below 100 m. On average, silicic acid concentrations were highest in the western basin of Bransfield Strait (Fig. 5f) and in Gerlache Strait, where the highest concentrations occurred in 2016 and 2017 (Fig. 5c). The highest silicic acid concentrations were observed in 2017 and the lowest in 2014 along the entire northern Antarctic Peninsula. However, silicic acid concentrations in 2017 were even higher,

macronutrient concentrations during positive SAM and ENSO years. The horizontal bars are the propagated uncertainties in calculating the difference between the averages for each depth and the *p*-values refer to the statistical tests to assess the significance of the difference between the average profiles.

and throughout the entire water column, in the central and eastern basins of Bransfield Strait (Fig. 5i,l) than in the western basin of Bransfield Strait and the Gerlache Strait (Fig. 5c,f), where this increase was more pronounced below 100 m. In the central basin of Bransfield Strait there was higher inter-annual variability and concentrations of DIN, which were higher in 2011 and 2018 (Fig. 5g), while across the entire northern Antarctic Peninsula they were higher in 2015 and lower in 2016. High interannual variability was also observed in phosphate concentrations of up to twofold ($\sim$ 1–3 μmol kg^{-1}) throughout the northern Antarctic Peninsula (second column in Fig. 5). The highest concentrations of phosphate were measured in 2003 in the Gerlache Strait (Fig. 5b), 2010 in the western basin of Bransfield Strait (Fig. 5e), and 2011 in the central basin of Bransfield Strait (Fig. 5h), and the lowest in 2008 in the eastern basin of Bransfield Strait (Fig. 5k) and 2014 in both Gerlache Strait (Fig. 5b) and the western basin of Bransfield Strait (Fig. 5e).

We compared the average profiles of macronutrients along the northern Antarctic Peninsula during periods of positive and negative SAM or ENSO (Fig. 6). In years of positive SAM, we observed highest (red line profiles on positive values in Fig. 6)

concentrations of DIN (first column in Fig. 6), phosphate (second column in Fig. 6), and silicic acid (third column in Fig. 6) through the water column along the northern Antarctic Peninsula. Such highest concentrations were more pronounced in silicic acid, mainly in the central (Fig. 6i) and eastern (Fig. 6l) basins of Bransfield Strait, particularly below 250 m. Phosphate and DIN concentrations were highest in all regions during summers of positive SAM. However, there was no significant difference in phosphate between years of positive and negative SAM in the central basin of Bransfield Strait (Fig. 6h). Furthermore, there was greater uncertainty in the phosphate difference in the Gerlache Strait (Fig. 6b), where the DIN was highest (Fig. 6a) but also not significant. Compared to SAM, there was a smaller difference in macronutrient concentrations between the years of positive and negative ENSO (blue line profiles in Fig. 6). Yet, larger differences were observed in the central (Fig. 6g–i) and eastern (Fig. 6j–l) basins of Bransfield Strait, where macronutrient concentrations were lower during positive ENSO. Silicic acid concentrations were lower during positive ENSO in all regions, but the differences were not significant. On the other hand, DIN concentration was significantly lower in the central (Fig. 6g) and eastern (Fig. 6j) basins of Bransfield Strait, while it was
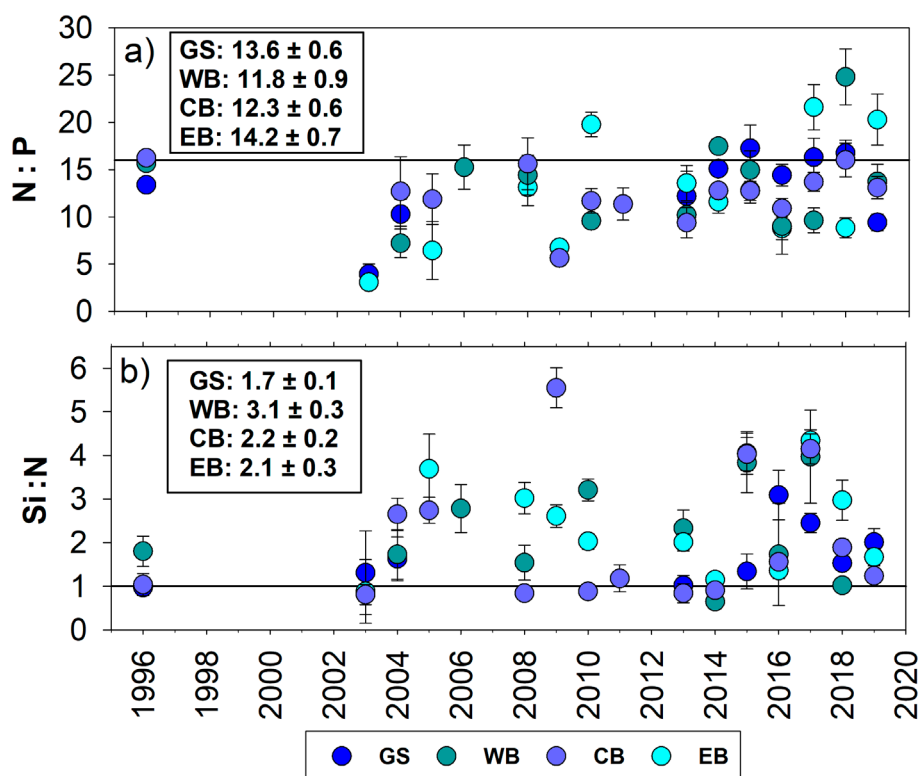

Fig. 7. Time series of macronutrient uptake stoichiometry. (**a**) DIN/phosphate (N : P) and (**b**) silicic acid/N (Si : N) uptake ratios during austral summer (January to March) along the northern Antarctic Peninsula. Colors show the subregions studied (CB, Central Bransfield; EB, Eastern Bransfield; GS, Gerlache Strait; WB, Western Bransfield). The vertical bars are the standard error on the slope of the regression N vs. P, and Si vs. N. Likewise, the values shown on the inset of each plot are the (**a**) N : P and (**b**) Si : N ratios with the respective standard deviations, considering the average profiles over the period for each region (Fig. 5). The solid black lines mark the ratios (**a**) N : P = 16 and (**b**) Si : N = 1. Statistics for each year are shown in Supporting Information Table S3.

significantly higher in the western basin (Fig. 6d). In addition, phosphate concentration was significantly higher during years of positive ENSO in the Gerlache Strait (Fig. 6b) and the western basin of Bransfield Strait (Fig. 6e), while it was lower in the eastern basin (Fig. 6k).

Uptake stoichiometry and seasonal drawdown of macronutrients

The full-depth average DIN/phosphate uptake ratio (hereafter N : P) across the northern Antarctic Peninsula environments ranged from 11.8 ± 0.9 ($r^2 = 0.965$; $p < 0.001$) to 14.2 ± 0.7 ($r^2 = 0.978$; $p < 0.001$), observed in the western and eastern basins of Bransfield Strait (Fig. 7a), respectively. From

2013 to 2019, when data are available for all northern Antarctic Peninsula environments, the lowest N : P uptake ratios (< 11) were observed in 2016 along the Bransfield Strait (Supporting Information Table S3), while in the Gerlache Strait the lowest N : P uptake ratio (9.40 ± 0.87; $r^2 = 0.95$; $p < 0.001$; $n = 8$) was recorded in 2019. N : P uptake ratios higher than 20 were observed in the western basin of Bransfield Strait in 2018 and in the eastern basin in 2017 and 2019. The average silicic acid/DIN uptake ratio (hereafter Si : N) ranged from 1.7 ± 0.1 ($r^2 = 0.974$; $p < 0.001$) in Gerlache Strait to 3.1 ± 0.3 ($r^2 = 0.956$; $p < 0.001$) in the western basin of Bransfield Strait (Fig. 7b). From 2013 to 2019, the lowest Si : N uptake ratio (< 1.2) was recorded in 2014 along the entire
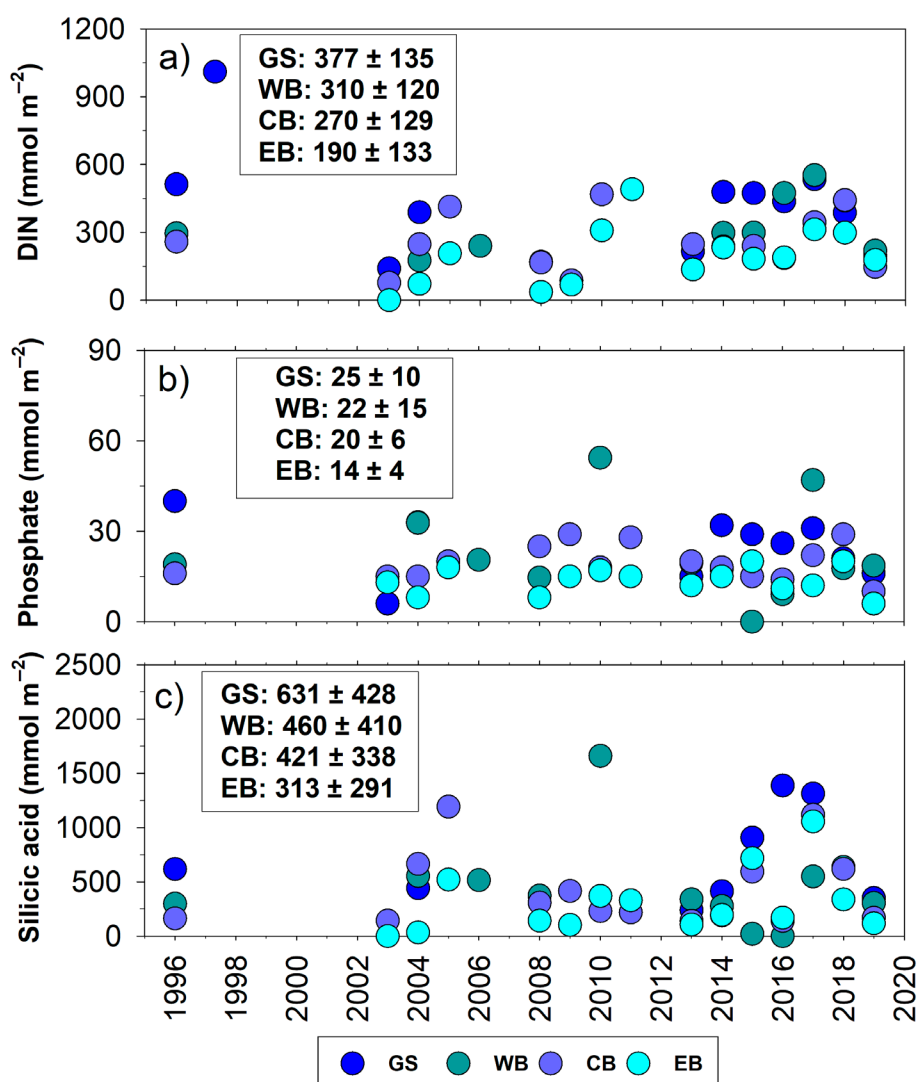
Fig. 8. Time series of seasonal nutrient drawdown. (**a**) DIN, (**b**) phosphate, and (**c**) silicic acid, during austral summer (January to March) along the northern Antarctic Peninsula. Each circle represents the seasonal drawdown of each nutrient for each year in Gerlache Strait (GS) and the western (WB), central (CB), and eastern (EB) basins of Bransfield Strait. The values shown on the inset are the averages for the entire period with the respective standard deviations.

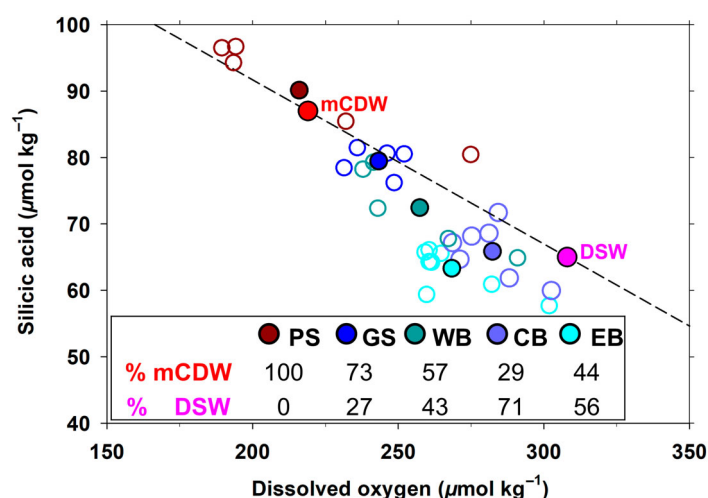**Fig. 9.** Influence of mixing between modified Circumpolar Deep Water (mCDW) and Dense Shelf Water (DSW) from the Weddell Sea on dissolved oxygen and silicic acid concentrations below 50 m along the northern Antarctic Peninsula. Open circles represent the average concentrations of dissolved oxygen and silicic acid for each depth interval below 50 m and closed circles indicate the average through the water column below 50 m at Palmer Station (PS), Gerlache Strait (GS) and the western (WB), central (CB), and eastern (EB) basins of Bransfield Strait. The data used here are from the profiles shown in Figs. 4, 5. For PS, we used dissolved oxygen (Waite 2022) and silicic acid (Ducklow et al. 2019) data from the U.S. Palmer Station (Fig. 1). The dissolved oxygen concentration endmembers were 219 μmol kg^{-1} for mCDW (red filled circle) and 308 μmol kg^{-1} for DSW (pink filled circle), from Damini et al. (2022). The silicic acid concentration endmembers were 87 μmol kg^{-1} (Cape et al. 2019) for mCDW and 65 μmol kg^{-1} (Hoppema et al. 2015) for DSW.

northern Antarctic Peninsula and the highest ratios (> 3.8) were recorded in 2015 and 2017 along Bransfield Strait. A Si : N uptake ratio of 5.5 ± 0.5 was recorded in 2009 in the central basin of Bransfield Strait, twofold the average for the entire period in that region (2.2 ± 0.2).

The seasonal drawdown in all macronutrients is characterized by a decreasing pattern from south (Gerlache Strait) to north (eastern basin of Bransfield Strait) along the northern Antarctic Peninsula (Fig. 8). High seasonal drawdown of phosphate was observed in 2010 in the western basin of Bransfield Strait, while higher drawdown of silicic acid was observed in 2016 and 2017 in Gerlache Strait. Seasonal drawdown of silicic acid close to zero was observed in 2015 and 2016 in the western basin of Bransfield Strait, where phosphate seasonal drawdown was close to zero in 2015, likely due to limitations in the estimation approach (*see* "Seasonal macronutrient drawdown" in "Discussion" section). The interannual variability (i.e., standard deviation) in drawdown of phosphate (Fig. 8b) and silicic acid (Fig. 8c) was high in the western basin of Bransfield Strait, while the variability in drawdown of DIN was fairly similar in all sub-regions along the northern Antarctic Peninsula (Fig. 8a).

Discussion

Main sources of macronutrients for the northern Antarctic Peninsula

The main source of macronutrients for northern Antarctic Peninsula environments is the Circumpolar Deep Water intrusions in the coastal and shelf south domains (Henley et al. 2019), which carry DIN, phosphate, and silicic acid (Figs. 2, 3) as this intermediate water is modified/mixing with upper waters and advected along the continental shelf northwards (Prézelin et al. 2000; Venables et al. 2017). When Circumpolar Deep Water intrudes at intermediate depths into the shelf domains (i.e., Gerlache Strait, and western basin of Bransfield Strait), it often upwells due to topographic effects (Venables et al. 2017; Parra et al. 2020) and transport macronutrients into surface waters. These waters are further advected northward by the Bransfield Current towards the eastern basin of Bransfield Strait, enriching the surface waters of the northern Antarctic Peninsula with high concentrations of macronutrients. Therefore, there is no evidence for macronutrient concentrations exhausted in the northern Antarctic Peninsula surface waters during summer, even in years with strong phytoplankton blooms (e.g., 2016; Costa et al. 2020, 2021). Indeed, high concentrations of summer chlorophyll *a* have been recorded along the northern Antarctic Peninsula (Ferreira et al. 2022) and several studies have shown that this region is not likely to experience iron limitation due to inputs from continental sources and icebergs (Ferreira et al. 2020 and references therein). Hence, the high concentrations of surface macronutrients along the northern Antarctic Peninsula are likely not associated with a limitation in primary production, but with the intense macronutrient supply from modified Circumpolar Deep Water. High sea surface concentrations of nitrate (12–24 μmol kg^{-1}) and phosphate (1.0–1.6 μmol kg^{-1}) are observed offshore south of the northern Antarctic Peninsula (Hauri et al. 2015), under strong influence of the Antarctic Circumpolar Current that carries Circumpolar Deep Water. Furthermore, high sea surface concentrations of DIN and phosphate (greater than 11.0 and 0.9 μmol kg^{-1}, respectively) were found during summer at Marian Cove in the central basin of Bransfield Strait, which was associated with the strong influence of modified Circumpolar Deep Water intrusions (Jones et al. 2023).

Although the modified Circumpolar Deep Water is also an important source of macronutrients for the coastal regions south of the northern Antarctic Peninsula (Prézelin et al. 2000; Henley et al. 2019), surface waters almost exhausted with respect to DIN and phosphate have been recorded in summer over the continental shelf in Marguerite Bay (Henley et al. 2017, 2018). However, along the northern Antarctic Peninsula, surface concentrations of DIN and phosphate were not lower than 15 and 0.5 μmol kg^{-1}, respectively (Fig. 5; Supporting Information Fig. S6a,d). This is likely because both the south zone of Gerlache Strait and the western basin of

Bransfield Strait are regions more exposed to the Antarctic Circumpolar Current influence, which probably facilitates more frequent intrusions of modified Circumpolar Deep Water (Anadón and Estrada 2002; Parra et al. 2020), favoring a greater supply of macronutrients into the surface layer through topographic upwelling and advective mixing. Indeed, in the Palmer Station region, in the southernmost part of the northern Antarctic Peninsula, modified Circumpolar Deep Water is expected to exert a strong and constant influence on macronutrient supply (Fig. 9; Prézelin et al. 2000; Kim et al. 2016). Along the northern Antarctic Peninsula average surface concentrations of silicic acid are higher than 50 μmol kg^{-1} (Fig. 5c,f,i,l) and in the southernmost part of the northern Antarctic Peninsula such concentrations can reach 100 μmol kg^{-1} (Supporting Information Fig. S8g). This is likely due to the local terrestrial sources of silicic acid in these regions (Hawkings et al. 2017), further supplementing the high silicic acid input from modified Circumpolar Deep Water (*see* section below). Indeed, the surface silicic acid concentration in the Palmer Station region (69.0 $\pm$ 10.4 μmol kg^{-1}; Supporting Information Fig. S8a) is higher than that found along the northern Antarctic Peninsula (third column in Fig. 5). In both regions, such concentrations are even higher than those found in the northwest Weddell Sea (Hoppema et al. 2015), where the direct influence of modified Circumpolar Deep Water is comparatively small.

Circumpolar Deep Water had a long period over which remineralized organic matter has accumulated and hence high concentrations of macronutrients. Along the northern Antarctic Peninsula, this is even more evident in the concentrations of phosphate (Fig. 2e) and silicic acid, whose concentrations are up to 50% higher under the influence of modified Circumpolar Deep Water in the Gerlache Strait and western basin of Bransfield Strait than in the rest of the northern Antarctic Peninsula (Fig. 2f). The central basin of Bransfield Strait is strongly influenced by Dense Shelf Water from the Weddell Sea in the deep layers (> 800 m; Dotto et al. 2016; Damini et al. 2022), where there are higher concentrations of DIN (Fig. 2d), phosphate (Fig. 2e), and dissolved oxygen (Fig. 2c) associated with lower concentrations of silicic acid (Figs. 2f, 9). This is a result of the slower rate of opal dissolution, as diatom frustules sink out of the surface layer, compared to the remineralization of sinking organic matter (Brown et al. 2006) that releases DIN and phosphate (Hoppema et al. 2015). Indeed, phytoplankton blooms recorded in the northwestern Weddell Sea are often composed mostly (> 80%) of diatoms (Mendes et al. 2012), associated with low N : P uptake ratios (< 14) and high Si : N ratios (>1; Flynn et al. 2021). Moreover, we found low N : P uptake ratios (< 16, Fig. 7a) and high Si : N uptake ratios (> 2, Fig. 7b) along the northern Antarctic Peninsula, although there is great interannual variability in these estimations. Due to the marked depletion of silicic acid during diatom growth, the Dense Shelf Water from the Weddell Sea is relatively low in silicic acid while the concentrations of DIN and phosphate are increased by remineralization of sinking

organic matter as it is advected towards the northern Antarctic Peninsula. The advection time of shelf waters from the Weddell Sea toward the Bransfield Strait is estimated to be between 1 and 5 months to reach the central basin (Van Caspel et al. 2018; Damini et al. 2022). This time is likely not long enough to release high silicic acid concentrations from late spring diatom blooms. Thus, the interannual variability in macronutrient concentrations driven by Dense Shelf Water advection is likely due to variability (i) in the residency time over shelves varying of around 3–6 years (Schlosser et al. 1991), (ii) in the advection time of these waters and (iii) in the timing and duration of diatom blooms, from early spring to summer. The influence of modified Circumpolar Deep Water and Dense Shelf Water from the Weddell Sea on silicic acid concentrations is most evident when we estimate the contribution of these waters along the northern Antarctic Peninsula from the silicic acid versus dissolved oxygen mixing diagram (Fig. 9). Below 50 m, the southern end of the northern Antarctic Peninsula (near Palmer Station) is strongly influenced by the silicic acid-rich and dissolved oxygen-poor modified Circumpolar Deep Water. Conversely, the central basin of Bransfield Strait is strongly influenced by the high dissolved oxygen and low silicic acid Dense Shelf Water. This west–east pattern in the fractional contributions of modified Circumpolar Deep Water and Dense Shelf Water to the total mixture is very close to the estimates determined by Damini et al. (2022) in the region. For the deep layers (i.e., > 800 m) of central basin of Bransfield Strait, those authors estimated an averaged contribution of 31% $\pm$ 9% of modified Circumpolar Deep Water and 69% $\pm$ 9% of Dense Shelf Water, while for the eastern basin of Bransfield Strait the averaged contribution to the mixture was 44% $\pm$ 8% for modified Circumpolar Deep Water and 56 $\pm$ 8 for Dense Shelf Water. Although the Palmer Station region is made up of almost 100% modified Circumpolar Deep Water below 50 m, silicic acid concentrations are higher than 87 μmol kg^{-1} (Fig. 9) expected only from modified Circumpolar Deep Water input (Cape et al. 2019), revealing that there are important local sources of silicic acid in this region.

Additional sources of macronutrients for the northern Antarctic Peninsula

Local sources of nutrients are known to be important along the northern Antarctic Peninsula. Terrestrial input of iron (De Jong et al. 2012; Ferreira et al. 2020) and silicic acid (Hawkings et al. 2017; Jones et al. 2023) is well known over the Antarctic continental shelf. However, remineralized macronutrients after intense phytoplankton blooms in fjords that flow into the northern Antarctic Peninsula (Forsch et al. 2021) can be injected into downstream regions, increasing DIN and phosphate concentrations (Jones et al. 2023). Moreover, the abrupt freshwater outflow from fjords increases the upper ocean stability and fertilizes the region with iron (Forsch et al. 2021), triggering intense phytoplankton blooms downstream. Likewise, such favorable conditions for intense

phytoplankton growth, mainly diatoms, are also triggered by glacial meltwater (Meredith et al. 2022; Jones et al. 2023) and sea ice melting (Mendes et al. 2018; Costa et al. 2020). Such high primary productivity sustains a high zooplankton density (Henley et al. 2019; Plum et al. 2020), which can increase the concentration of remineralized macronutrients locally and downstream via sloppy feeding (Ratnarajah and Bowie 2016), as well as intensifying the recycling of organic matter (Avelina et al. 2020) at their resting depths by respiration and throughout their depth habitat range by fecal pellet production (Whitehouse et al. 2011; Henley et al. 2020). Furthermore, the eastern basin of Bransfield Strait is an important pathway of icebergs released from the Weddell Sea (Collares et al. 2018; Barbat and Mata 2021), which transport iron (Laufkötter et al. 2018) and likely silicic acid (Hawkings et al. 2017) from the eastern shelf of the Antarctic Peninsula into the northern Antarctic Peninsula. Hence, there is an increased supply of silicic acid in the eastern basin of Bransfield Strait (Fig. 2f), where there are also episodic intrusions of silicic acid-enriched modified Circumpolar Deep Water at intermediate levels (Dotto et al. 2016; Damini et al. 2022). Although widely neglected in biogeochemical studies, mesoscale eddies may have a relevant impact on nutrient supply along the northern Antarctic Peninsula. Such structures can favor nutrient supply via upwelling of waters enriched with remineralized material (Damini et al. 2023) and by intensifying remineralization by deepening the mixed layer depth within the eddies (Dufois et al. 2014; Damini et al. 2023). Moreover, eddies can trap advected water masses (Damini et al. 2023) with high remineralized nutrient content (Dufois et al. 2014), such as modified Warm Deep Water (a mixture of Circumpolar Deep Water with Winter Water in the Weddell Sea; Hoppema et al. 2015).

The high concentration of macronutrients (Fig. 2) and the supply of iron (Ardelan et al. 2010) coupled with the increased upper ocean stability driven by sea ice melting and/or glacial freshwater input during the summer supports high productivity along the northern Antarctic Peninsula (Mendes et al. 2018; Costa et al. 2020). We found an average N : P uptake ratio (Fig. 7a) within the expected range for the northern Antarctic Peninsula ($\sim$ 13–21; Henley et al. 2019), but with a high interannual variability, as well as N : P and Si : N uptake ratios, suggest that there are different dominant groups in phytoplankton blooms over interannual scales. In the Southern Ocean, lower N : P uptake ratios (< 16) have been observed during diatom blooms, while other smaller phytoplankton groups are associated with a higher (> 16) ratio (Arrigo et al. 1999; Henley et al. 2019, 2020). This is particularly true along the northern Antarctic Peninsula, where we observed low N : P uptake ratios (< 16, Fig. 7a) when the phytoplankton assemblage was dominated by diatoms (Supporting Information Fig. S9). For example, a low N : P uptake ratio was observed in 2016 along the northern Antarctic Peninsula (Supporting Information Table S3), when an intense phytoplankton bloom was recorded

(Costa et al. 2020, 2021) and over 90% of it was composed of diatoms (Supporting Information Fig. S9). Conversely, there were high N : P uptake ratios (> 20; Supporting Information Fig. 7a) in 2017 along the northern Antarctic Peninsula and in 2018 in the western basin of Bransfield Strait, when phytoplankton composition was dominated by other smaller groups, such as dinoflagellates, haptophytes (*Phaeocystis antarctica*), cryptophytes and green flagellates (Supporting Information Fig. S9). However, we found even lower N : P uptake ratios (< 9) in some years (Fig. 7a), indicating possible additional sources of phosphate in relation to DIN. This may be associated with the release of phosphate accumulated in sea ice (Fripiat et al. 2017), although its effect on the water column remains unclear (Henley et al. 2019). Moreover, the high density of krill enriched by diatom blooms (Henley et al. 2020) may favor phosphate resupply, as krill release phosphate and ammonium through grazing and excretion processes (Tovar-Sanchez et al. 2007). We identified Si : N uptake ratios that were within the range previously observed south of the northern Antarctic Peninsula (1–3; Kim et al. 2016; Henley et al. 2019). Si : N uptake ratios higher than 1 have been associated with diatoms growing under iron-limited conditions (Takeda 1998; Henley et al. 2020), but the northern Antarctic Peninsula is not expected to experience iron limitation (De Jong et al. 2012; Ferreira et al. 2020 and references therein). The higher Si : N uptake ratios are likely to be a result of high silicic acid concentrations being supplied by modified Circumpolar Deep Water intrusions and additional sources of silicic acid such as local remineralization/dissolution of diatoms walls and mainly terrestrial inputs (Hawkings et al. 2017; Jones et al. 2023). The intense diatom blooms in early spring can lead to a depletion in silicic acid in the upper ocean (Kim et al. 2016) and then opal dissolution increases the silicic acid concentration again toward late summer. Indeed, we found the highest Si : N ratio and the lowest N : P ratio in the western basin of Bransfield Strait (Fig. 7), where there is a great influence of modified Circumpolar Deep Water intrusions (Fig. 2) and intense diatom-dominated blooms (Anadón and Estrada 2002; Costa et al. 2020).

Drivers of interannual variability of macronutrients along the northern Antarctic Peninsula

The huge interannual variability in nutrient concentrations along the northern Antarctic Peninsula is driven mainly by the relative strength of modified Circumpolar Deep Water intrusions and the advection of Dense Shelf Water from the Weddell Sea. During positive SAM, westerly winds are intensified southward (Marshall et al. 2006), strengthening modified Circumpolar Deep Water intrusions along the northern Antarctic Peninsula (Barlett et al. 2018; Damini et al. 2022) and increasing nutrient concentration. In addition to direct nutrient input, greater vertical mixing leads to an increased supply of organic matter (da Cunha et al. 2018; Avelina et al. 2020) and a consequent increase in remineralized nutrient concentrations throughout the water column. Overall, the influence

of SAM on nutrient concentrations is more evident in the central and eastern basins of Bransfield Strait because these regions are more influenced by Dense Shelf Water from the Weddell Sea than both the western basin of Bransfield Strait and Gerlache Strait (Barlett et al. 2018; Damini et al. 2022). In these regions, greater differences between positive and negative SAM are observed in silicic acid concentrations because Dense Shelf Water (modified Circumpolar Deep Water) is depleted (enriched) in silicic acid (Fig. 9). During events of positive SAM, Dense Shelf Water advection into Bransfield Strait is weakened, while modified Circumpolar Deep Water intrusion is strengthened (Wang et al. 2022), increasing the difference in influence of these distinct water masses. On the other hand, the influence of Dense Shelf Water is smaller in the western basin of Bransfield Strait and the Gerlache Strait (Wang et al. 2022), decreasing the silicic acid dilution due to Dense Shelf Water advection. This is supported by the smaller influence of SAM on phosphate and DIN concentrations in Gerlache Strait (Fig. 6), as the time for organic matter remineralisation (on a timescale of days; Brown et al. 2006; Hoppema et al. 2015) is likely shorter than the advection time for Dense Shelf Water to reach this region (on a timescale of months; Van Caspel et al. 2018; Damini et al. 2022).

Conversely, during events of positive ENSO, westerly winds typically migrate northward (Stammerjohn et al. 2008) and weaken modified Circumpolar Deep Water intrusions over the northern Antarctic Peninsula (Barlett et al. 2018; Damini et al. 2022), decreasing nutrient supply. Such conditions increase the extent of the Dense Shelf Water advected from the Weddell Sea, reaching the southern end of the northern Antarctic Peninsula (i.e., Gerlache Strait, Wang et al. 2022). Since Dense Shelf Water is enriched in DIN and phosphate (Fig. 2d,e) and contains lower concentrations of silicic acid than modified Circumpolar Deep Water (Fig. 2f), the interannual variability in silicic acid concentrations is intensified over the northern Antarctic Peninsula. Indeed, we observed a 57% decrease in average silicic acid concentration from 2015 (a year of positive SAM) to 2016 (a year of strong positive ENSO) in the central basin of Bransfield Strait, where significant changes were also observed in organic carbon concentrations between these two years (Avelina et al. 2020). The influence of ENSO on DIN and phosphate concentrations is minor compared to SAM (Fig. 6) because Dense Shelf Water also contains high concentrations of these nutrients. Moreover, variations in ENSO are expected to exert less influence on circulation along the northern Antarctic Peninsula than variations in SAM (Wang et al. 2022). This may be associated with uncertainties in the circulation response time to ENSO variations (i.e., 6–9 months; Barlett et al. 2018; Dotto et al. 2016) and Dense Shelf Water advection time along the northern Antarctic Peninsula, which are still a challenge to understand. The Dense Shelf Water is estimated to take around 1–5 months to reach the central basin of Bransfield Strait from the northwestern Weddell Sea (Van Caspel

et al. 2018; Damini et al. 2022). The period of around 5 months is consistent with the estimated time for the drift of medium-sized icebergs from the northwestern Weddell Sea to reach the central basin of Bransfield Strait (Collares et al. 2018). However, its interannual variability and sensitivity to SAM and ENSO events, as well as the residence time of the waters within Bransfield Strait remain unclear. Macronutrient concentrations appear to be more sensitive to ENSO in the eastern basin of Bransfield Strait (Fig. 6) because this is the main pathway of Dense Shelf Water input into the northern Antarctic Peninsula (Van Caspel et al. 2018; Wang et al. 2022). Therefore, it is reasonable to conclude that the high interannual variability in nutrient concentrations along the northern Antarctic Peninsula is driven mainly by changes in ocean circulation and water mass mixing caused by strong variability in the SAM. The effect of ENSO variability on silicic acid concentrations via advected Dense Shelf Water is more evident while its effect on DIN and phosphate concentrations is often counteracted because DIN and phosphate are also high in Dense Shelf Water.

In addition, the effects of SAM and ENSO on the biogeochemistry of waters along the northern Antarctic Peninsula can either reinforce or counteract each other, depending on whether the region experiences concomitant periods of both positive SAM and ENSO or vice versa (Stammerjohn et al. 2008). Since the interannual variability of macronutrients is driven mainly by the influence of SAM compared to ENSO, during combined years of both positive SAM and ENSO macronutrients concentrations are expected to remain high along the northern Antarctic Peninsula. Indeed, we observed concentrations within the standard deviation for all macronutrients in 2004, 2010, and 2019 (Fig. 5), when the SAM and ENSO events were concomitantly positive (Table S2). Conversely, during combined years of both negative SAM and ENSO, lower concentrations of macronutrients are expected, as both intrusions of modified Circumpolar Deep Water (the main source of macronutrients) and the advection of Dense Shelf Water are weakened. However, regarding our results, unfortunately, we could not accurately assess these combined effects because we only have a more robust time series in the last decade when the Southern Ocean has been experiencing successive positive SAM (Keppler and Landschützer 2019) and negative ENSO conditions (Barlett et al. 2018). Although it is unclear what the additional sources were for the anomalous high concentrations of silicic acid in 2017, mainly in the central and eastern basins of Bransfield Strait (Fig. 5), these could be linked to an offset in the data or processes triggered by extreme events, such as glacier calving in the vicinity (Meredith et al. 2022), which need to be better understood. Indeed, it is more likely that these higher values are driven by an additional source of silicic acid, as similarly silicic acid concentrations as high as 110 μmol kg^{-1} were already observed in the central basin of the Bransfield Strait in the 1980s (Heywood and Priddle 1987), and near Ryder Bay in 2020 (Jones et al. 2023).

Seasonal macronutrient drawdown

Despite the high concentration of macronutrients that we observed throughout the northern Antarctic Peninsula environments, supporting high primary productivity, Gerlache Strait and the western basin of Bransfield Strait appear to be the most favorable regions for strong phytoplankton growth. Seasonal nutrient drawdown in these regions is nearly double that observed in the rest of the northern Antarctic Peninsula (Fig. 8). There is a clear south–north decreasing gradient in seasonal nutrient drawdown along the northern Antarctic Peninsula. Even in the Gerlache Strait, where the seasonal drawdown is higher (Fig. 8), it is lower than that found in the Palmer Station region (Kim et al. 2016) and further south at Marguerite Bay (Henley et al. 2017, 2018). The situation of macronutrients being completely replenished in the upper mixed layer was observed in 2003 for silicic acid in the Gerlache Strait, and in the western basin of Bransfield Strait in 2015 for phosphate and in 2015 and 2016 for silicic acid. This may reflect a limitation of our approach to estimating seasonal drawdown, mainly due to variations in the upper mixed layer depth or the influence of vertical mixing, since the minimum temperature between 50 and 100 m in summer is on average around 1.0°C higher than the Winter Water, reflecting its modification by mixing with other water masses. Nevertheless, the relatively lower seasonal drawdown of macronutrients (Fig. 8) along the northern Antarctic Peninsula, compared with the Palmer Station region (Kim et al. 2016), may be due to greater vertical mixing in these environments during the productive summer period, such as the central and eastern basins of Bransfield Strait compared to the south areas of northern Antarctic Peninsula (Wang et al. 2022). Low seasonal drawdown may also be due to the rapid regeneration of macronutrients in the upper mixed layer, mainly DIN and phosphate, as already observed at Marguerite Bay (Henley et al. 2018).

As Gerlache Strait and the western basin of Bransfield Strait are shallower, more enclosed areas, and closer to the coast, they are more likely to experience increased upper ocean stability as a result of sea ice melting and glacial freshwater input. Such conditions are favorable to phytoplankton blooms (Costa et al. 2020; Ferreira et al. 2022) and, therefore, to greater seasonal drawdown of macronutrients. As the summer phytoplankton blooms in these regions are dominated by diatoms (Costa et al. 2020, 2021; Ferreira et al. 2022), which are known to enhance CO_2 uptake (Costa et al. 2020; Henley et al. 2020), these regions also act as a strong summer atmospheric CO_2 sink (Monteiro et al. 2020a,b). The dominance of phytoplankton growth either by diatoms or smaller cells was thought to act as an additional controlling factor for the magnitude of CO_2 uptake in Gerlache Strait (Kerr et al. 2018c). In fact, the highest seasonal drawdown of silicic acid was recorded in Gerlache Strait in 2016 (Fig. 8c), when there was an intense diatom bloom (Costa et al. 2020) and the strongest summer CO_2 uptake since 1999 (Monteiro

et al. 2020a,b). The great interannual variability in seasonal nutrient drawdown must also be driven to some extent by winter sea ice cover (Kim et al. 2016; Henley et al. 2017). During the negative SAM condition, increased winter sea ice cover enhances the upper ocean stability driving phytoplankton blooms in the following summer (Saba et al. 2014), increasing the seasonal nutrient drawdown (Kim et al. 2016). Moreover, diatom blooms can be enhanced significantly by the release of diatom cells from the sea ice during intense ice melting during summer (Kim et al. 2016). Hence, part of the high interannual variability in nutrient concentration associated with the SAM and ENSO along the northern Antarctic Peninsula must be driven by the variation in sea ice extent, which is also driven by these climate modes.

Conclusions

High concentrations of macronutrients (DIN, phosphate, and silicic acid) were recorded during austral summers from 1996 to 2019 in environments along the northern Antarctic Peninsula. In particular, the upper ocean minimum concentrations of DIN (16 μmol kg^{-1}), phosphate (0.7 μmol kg^{-1}), and silicic acid (50 μmol kg^{-1}) along the northern Antarctic Peninsula are higher than those commonly recorded south of the northern Antarctic Peninsula (e.g., over the continental shelf at Marguerite Bay) where DIN and phosphate almost exhausted have been recorded. The macronutrient concentrations exhibited huge interannual variability, with up to threefold changes in silicic acid and twofold changes in phosphate concentrations among the annually averaged profiles for each region. The coupling of modified Circumpolar Deep Water intrusions together with local sources, such as remineralization of organic matter, terrigenous inputs of silicic acid, mesoscale structures and circulation, and sea ice dynamics, explains the high nutrient concentrations found along the northern Antarctic Peninsula. The great interannual variability is also driven largely by the extent of modified Circumpolar Deep Water intrusions and it's mixing with the Dense Shelf Water advected from the Weddell Sea. The strength of modified Circumpolar Deep Water intrusions, and hence nutrient supply, is often modulated by the SAM, and to a lesser extent by ENSO. However, further studies are needed to better distinguish and decouple the influence of these climate modes on changes in the mixing dynamics between modified Circumpolar Deep Water and Dense Shelf Water, which was not possible in our study because positive SAM events prevail over the last two decades. We recommend that future studies aim to understand the net effect of the coupling of SAM and ENSO in their positive and negative phases on the biogeochemistry of this climatically sensitive region.

We found stoichiometric uptake ratios of N : P less than 16 and Si : N greater than 1, associated with high phytoplankton biomass, mainly composed of diatoms, which have been associated to strong CO_2 uptake in the coastal and relatively

shallow zone of the northern Antarctic Peninsula. Despite the enhanced summer phytoplankton growth, relatively low seasonal nutrient drawdown was found in most subregions of the northern Antarctic Peninsula. This is likely due to the large supply of macronutrients from different sources, which makes northern Antarctic Peninsula environments highly favorable for growth and development of phytoplankton blooms. This is particularly important as the northern Antarctic Peninsula is one of the most productive regions in the Southern Ocean and where major climate-driven change is being observed. Hence, these findings are critical to improving our understanding of the natural variability of Southern Ocean ecosystems and informing our predictions of how these nutrient inputs may respond to ongoing and expected climate and environmental change.

Data Availability Statement

The data that support the findings of this study are published as the product BGQNAPv1.0: A summer macronutrients binned data set for the Northern Antarctic Peninsula, Southern Ocean, openly at https://doi.org/10.5281/zenodo.7384423 (Monteiro et al. 2022).

References

Aminot, A., and M. Chaussepied. 1983. Manuel des analyses chimiques en milieu marin. Centre National pour L'Exploitation des Oceans. CNEXO.

Anadón, R., and M. Estrada. 2002. The FRUELA cruises: A carbon flux study in productive areas of the Antarctic Peninsula (December 1995–February 1996). Deep Sea Res. II Top. Stud. Oceanogr. **49**: 567–583. doi:10.1016/S0967-0645(01)00112-6

Ardelan, M. V., O. Holm-Hansen, C. D. Hewes, C. S. Reiss, N. S. Silva, H. Dulaiova, E. Steinnes, and E. Sakshaug. 2010. Natural iron enrichment around the Antarctic Peninsula in the Southern Ocean. Biogeosciences **7**: 11–25. doi:10.5194/bg-7-11-2010

Arrigo, K. R., D. H. Robinson, D. L. Worthen, R. B. Dunbar, G. R. Ditullio, M. Vanwoert, and M. P. Lizotte. 1999. Phytoplankton community structure and the drawdown of nutrients and CO_2 in the Southern Ocean. Science **283**: 365–367. doi:10.1126/science.283.5400.365

Avelina, R., L. C. da Cunha, C. d. O. Farias, C. Hamacher, R. Kerr, and M. M. Mata. 2020. Contrasting dissolved organic carbon concentrations in the Bransfield Strait, northern Antarctic Peninsula: Insights into El Niño–Southern Oscillation and Southern Annular Mode effects. J. Mar. Syst. **212**: 103457 10.1016/j.jmarsys.2020.103457

Barbat, M. M., and M. M. Mata. 2021. Iceberg drift and melting rates in the northwestern Weddell Sea, Antarctica: Novel automated regional estimates through machine learning. An. Acad. Bras. Ciênc. **94**: e20211586. doi:10.1590/0001-3765202220211586

Barlett, E. M. R., G. V. Tosonotto, A. R. Piola, M. E. Sierra, and M. M. Mata. 2018. On the temporal variability of intermediate and deep waters in the Western Basin of the Bransfield Strait. Deep Sea Res. II Top. Stud. Oceanogr. **149**: 31–46. doi:10.1016/j.dsr2.2017.12.010

Brown, L., R. Sanders, and G. Savidge. 2006. Relative mineralisation of C and Si from biogenic particulate matter in the upper water column during the Northeast Atlantic diatom bloom in spring 2001. J. Mar. Syst. **63**: 79–90. doi:10.1016/j.jmarsys.2006.03.001

Cape, M. R., and others. 2019. Circumpolar deep water impacts glacial meltwater export and coastal biogeochemical cycling along the West Antarctic Peninsula. Front. Mar. Sci. **6**: 144. doi:10.3389/fmars.2019.00144

Collares, L. L., M. M. Mata, R. Kerr, J. Arigony-Neto, and M. M. Barbat. 2018. Iceberg drift and ocean circulation in the northwestern Weddell Sea, Antarctica. Deep Res. II Top. Stud. Oceanogr. **149**: 10–24. doi:10.1016/j.dsr2.2018.02.014

Costa, R. R., C. R. B. Mendes, V. M. Tavano, T. S. Dotto, R. Kerr, T. Monteiro, C. Odebrecht, and E. R. Secchi. 2020. Dynamics of an intense diatom bloom in the Northern Antarctic Peninsula, February 2016. Limnol. Oceanogr. **66**: 1–20. doi:10.1002/lno.11437

Costa, R. R., C. R. B. Mendes, A. Ferreira, V. M. Tavano, T. S. Dotto, and E. R. Secchi. 2021. Large diatom bloom off the Antarctic Peninsula during cool conditions associated with 2015/2016 El Niño. Commun. Earth Environ. **2**: 252. doi:10.1038/s43247-021-00322-4

Costa, R. R., and others. 2023. Physical-biological drivers modulating phytoplankton seasonal succession along the Northern Antarctic Peninsula. Environ. Res. **231**: 116273. doi:10.1016/j.envres.2023

da Cunha, L. C., C. Hamacher, C.d. O. Farias, R. Kerr, C. R. B. Mendes, and M. M. Mata. 2018. Contrasting end-summer distribution of organic carbon along the Gerlache Strait, Northern Antarctic Peninsula: Bio-physical interactions. Deep Sea Res. II Top. Stud. Oceanogr. **149**: 206–217. doi:10.1016/j.dsr2.2018.03.003

Damini, B. Y., R. Kerr, T. S. Dotto, and M. M. Mata. 2022. Long-term changes on the Bransfield Strait deep water masses: Variability, drivers and connections with the northwestern Weddell Sea. Deep Sea Res. I Oceanogr. Res. Pap. **179**: 103667. doi:10.1016/j.dsr.2021.103667

Damini, B. Y., R. R. Costa, T. S. Dotto, C. R. B. Mendes, J. C. Torres-Lasso, M. d. V. C. Azaneu, M. M. Mata, and R. Kerr. 2023. Antarctica Slope Front bifurcation eddy: A stationary feature influencing CO_2 dynamics in the northern Antarctic Peninsula. Prog. Oceanogr. **212**: 102985. doi:10.1016/j.pocean.2023.102985

de Baar, H. J. W., J. T. M. De Jong, D. C. E. Bakker, B. M. Löscher, C. Veth, U. Bathmann, and V. Smetacek. 1995.

Importance of iron for plankton blooms and carbon dioxide drawdown in the Southern Ocean. Nature **373**: 412–415. doi:10.1038/373412a0

De Jong, J., V. Schoemann, D. Lannuzel, P. Croot, H. De Baar, and J.-L. Tison. 2012. Natural iron fertilization of the Atlantic sector of the Southern Ocean by continental shelf sources of the Antarctic Peninsula. J. Geophys. Res. Biogeosci. **117**: G01029. doi:10.1029/2011JG001679

Dotto, T. S., R. Kerr, M. M. Mata, and C. A. Garcia. 2016. Multidecadal freshening and lightening in the deep waters of the Bransfield Strait, Antarctica. J. Geophys. Res. Oceans **121**: 3741–3756. doi:10.1002/2015JC011228

Dotto, T. S., M. M. Mata, R. Kerr, and C. A. Garcia. 2021. A novel hydrographic gridded data set for the Northern Antarctic Peninsula. Earth Syst. Sci. Data **13**: 671–696. doi:10.5194/essd-13-671-2021

Dufois, F., N. J. Hardman-Mountford, J. Greenwood, A. J. Richardson, M. Feng, S. Herbette, and R. Matear. 2014. Impact of eddies on surface chlorophyll in the South Indian Ocean. J. Geophys. Res. Oceans **119**: 8061–8077. doi:10.1002/2014JC010164

Ferreira, A., R. R. Costa, T. S. Dotto, R. Kerr, V. M. Tavano, A. C. Brito, V. Brotas, E. R. Secchi, and C. R. B. Mendes. 2020. Changes in phytoplankton communities along the Northern Antarctic Peninsula: Causes, impacts and research priorities. Front. Mar. Sci. **7**: 576254. doi:10.3389/fmars.2020.576254

Ferreira, A., A. C. Brito, C. R. B. Mendes, V. Brotas, R. R. Costa, C. V. Guerreiro, C. Sá, and T. Jackson. 2022. OC4-SO: A new chlorophyll-a algorithm for the Western Antarctic Peninsula using multi-sensor satellite data. Remote Sens. **14**: 1052. doi:10.3390/rs14051052

Ferreira, M. L. C., and R. Kerr. 2017. Source water distribution and quantification of North Atlantic deep water and Antarctic bottom water in the Atlantic Ocean. Prog. Oceanogr. **153**: 66–83. doi:10.1016/j.pocean.2017.04.003

Flynn, R. F., T. G. Bornman, J. M. Burger, S. Smith, K. A. M. Spence, and S. E. Fawcett. 2021. Summertime productivity and carbon export potential in the Weddell Sea, with a focus on the waters adjacent to Larsen C Ice Shelf. Biogeosciences **18**: 6031–6059. doi:10.5194/bg-18-6031-2021

Forsch, K. O., L. Hahn-Woernle, R. M. Sherrell, V. J. Roccanova, K. Bu, D. Burdige, M. Vernet, and K. A. Barbeau. 2021. Seasonal dispersal of fjord meltwaters as an important source of iron and manganese to coastal Antarctic phytoplankton. Biogeosciences **18**: 6349–6375. doi:10.5194/bg-18-6349-2021

Fripiat, F., and others. 2017. Macro-nutrient concentrations in Antarctic pack ice: Overall patterns and overlooked processes. Elementa Sci. Anthropocene **5**: 13. doi:10.1525/elementa.217

Hauri, C., S. C. Doney, T. Takahashi, M. Erickson, G. Jiang, and H. W. Ducklow. 2015. Two decades of inorganic carbon dynamics along the West Antarctic Peninsula. Biogeosciences **12**: 6761–6779. doi:10.5194/bg-12-6761-2015

Hawkings, J., J. Wadham, L. Benning, K. R. Hendry, M. Tranter, A. Tedstone, P. Nienow, and R. Raiswell. 2017. Ice sheets as a missing source of silica to the polar oceans. Nat. Commun. **8**: 14198. doi:10.1038/ncomms14198

Henley, S. F., R. E. Tuerena, A. L. Annett, A. E. Fallick, M. P. Meredith, H. J. Venables, A. Clarke, and R. S. Ganeshram. 2017. Macronutrient supply, uptake and recycling in the coastal ocean of the west Antarctic Peninsula. Deep Sea Res. II Top. Stud. Oceanogr. **139**: 58–76. doi:10.1016/j.dsr2.2016.10.003

Henley, S. F., E. J. Jones, H. J. Venables, M. P. Meredith, Y. L. Firing, R. Dittrich, S. Heiser, J. Stefels, and J. Dougans. 2018. Macronutrient and carbon supply, uptake and cycling across the Antarctic Peninsula shelf during summer. Philos. Trans. R. Soc. A Math. Phys. Eng. Sci. **376**: 20170168. doi:10.1098/rsta.2017.0168

Henley, S. F., and others. 2019. Variability and change in the west Antarctic Peninsula marine system: Research priorities and opportunities. Prog. Oceanogr. **173**: 208–237. doi:10.1016/j.pocean.2019.03.003

Henley, S. F., and others. 2020. Changing biogeochemistry of the Southern Ocean and its ecosystem implications. Front. Mar. Sci. **7**: 581. doi:10.3389/fmars.2020.00581

Heywood, R. B., and J. Priddle. 1987. Retention of phytoplankton by an eddy. Cont. Shelf Res. **7**: 937–955. doi:10.1016/0278-4343(87)90007-0

Hoppema, M., K. Bakker, S. M. A. C. van Heuven, J. C. van Ooijen, and H. J. de Baar. 2015. Distributions, trends and inter-annual variability of nutrients along a repeat section through the Weddell Sea (1996–2011). Mar. Chem. **177**: 545–553. doi:10.1016/j.marchem.2015.08.007

Jones, R. L., and others. 2023. Continued glacial retreat linked to changing macronutrient supply along the West Antarctic Peninsula. Mar. Chem. **251**: 104230. doi:10.1016/j.marchem.2023.104230

Keppler, L., and P. Landschützer. 2019. Regional wind variability modulates the Southern Ocean carbon sink. Sci. Rep. **9**: 7384. doi:10.1038/s41598-019-43826-y

Kerr, R., M. M. Mata, C. R. B. Mendes, and E. R. Secchi. 2018*a*. Northern Antarctic Peninsula: A marine climate hotspot of rapid changes on ecosystems and ocean dynamics. Deep Res. II Top. Stud. Oceanogr. **149**: 4–9. doi:10.1016/j.dsr2.2018.05.006

Kerr, R., C. Goyet, L. C. da Cunha, I. B. M. Orselli, J. M. Lencina-Avila, C. R. B. Mendes, M. Carvalho-Borges, M. M. Mata, and V. M. Tavano. 2018*b*. Carbonate system properties in the Gerlache Strait, Northern Antarctic Peninsula (February 2015): II. Anthropogenic CO_2 and seawater acidification. Deep. Res. II. Top. Stud. Oceanogr. **149**: 182–192. doi:10.1016/j.dsr2.2017.07.007

Kerr, R., I. B. M. Orselli, J. M. Lencina-Avila, R. T. Eidt, C. R. B. Mendes, L. C. da Cunha, C. Goyet, M. M. Mata, and V. M.

Tavano. 2018*c*. Carbonate system properties in the Gerlache Strait, Northern Antarctic Peninsula (February 2015): I. Sea–air CO_2 fluxes. Deep Sea Res. II Top. Stud. Oceanogr. **149**: 171–181. doi:10.1016/j.dsr2.2017.02.008

Kim, H., S. C. Doney, R. A. Iannuzzi, M. P. Meredith, D. G. Martinson, and H. W. Ducklow. 2016. Climate forcing for dynamics of dissolved inorganic nutrients at Palmer Station, Antarctica: An interdecadal (1993–2013) analysis. J. Geophys. Res. Biogeosci. **121**: 2369–2389. doi:10.1002/2015JG003311

Laufkötter, C., A. A. Stern, J. G. John, C. A. Stock, and J. P. Dunne. 2018. Glacial iron sources stimulate the Southern Ocean carbon cycle. Geophys. Res. Lett. **13**: 385. doi:10.1029/2018GL079797

Lencina-Avila, J. M., C. Goyet, R. Kerr, I. B. M. Orselli, M. M. Mata, and F. Touratier. 2018. Past and future evolution of the marine carbonate system in a coastal zone of the Northern Antarctic Peninsula. Deep Sea Res. II Top. Stud. Oceanogr. **149**: 193–205. doi:10.1016/j.dsr2.2017.10.018

Marshall, G. J., A. Orr, N. P. M. van Lipzig, and J. C. King. 2006. The impact of a changing Southern Hemisphere annular mode on Antarctic Peninsula summer temperatures. J. Clim. **19**: 5388–5404. doi:10.1175/JCLI3844.1

Mata, M. M., V. M. Tavano, and C. A. E. García. 2018. 15 Years sailing with the Brazilian High Latitude Oceanography Group (GOAL). Deep Res. Top. Stud. Oceanogr. **149**: 1–3. doi:10.1016/j.dsr2.2018.05.007

Mendes, C. R. B., M. S. de Souza, V. M. T. Garcia, M. C. Leal, V. Brotas, and C. A. E. Garcia. 2012. Dynamics of phytoplankton communities during late summer around the tip of the Antarctic Peninsula. Deep Sea Res. I Oceanogr. Res. Pap. **65**: 1–14. doi:10.1016/j.dsr.2012.03.002

Mendes, C. R. B., V. M. Tavano, R. Kerr, T. S. Dotto, T. Maximiano, and E. R. Secchi. 2018. Impact of sea ice on the structure of phytoplankton communities in the northern Antarctic Peninsula. Deep Sea Res. II Top. Stud. Oceanogr. **149**: 111–123. doi:10.1016/j.dsr2.2017.12.003

Meredith, M. P., and others. 2022. Internal tsunamigenesis and ocean mixing driven by glacier calving in Antarctica. Sci. Adv. **8**: eadd0720. doi:10.1126/sciadv.add0720

Moffat, C., and M. Meredith. 2018. Shelf–ocean exchange and hydrography west of the Antarctic peninsula: A review. Philos. Trans. R. Soc. A Math. Phys. Eng. Sci. **376**: 20170164. doi:10.1098/rsta.2017.0164

Monteiro, T., R. Kerr, and E. da Costa Machado. 2020*a*. Seasonal variability of net sea-air CO_2 fluxes in a coastal region of the northern Antarctic Peninsula. Sci. Rep. **10**: 14875 10.1038/s41598-020-71814-0

Monteiro, T., R. Kerr, I. B. M. Orselli, and J. M. Lencina-Avila. 2020*b*. Towards an intensified summer CO2 sink behaviour in the Southern Ocean coastal regions. Prog. Oceanogr. **183**: 102267. doi:10.1016/j.pocean.2020.102267

Monteiro, T., R. Kerr, R. C. G. Pollery, C. R. B. Mendes, S. Henley, V. M. Tavano, C. A. E. Garcia, and M. M. Mata.

2022. BGQ Northern Antarctic Peninsula v1.0: A summer macronutrients binned data set for the Northern Antarctic Peninsula, Southern Ocean (1.0) [Data set]. Zenodo. 10.5281/zenodo.7384423

Olsen, A., and others. 2020. An updated version of the global interior ocean biogeochemical data product, GLODAPv2.2020. Earth Syst. Sci. Data **12**: 3653–3678. doi:10.5194/essd-12-3653-2020

Orselli, I. B. M., and others. 2022. The marine carbonate system along the northern Antarctic Peninsula: Current knowledge and future perspectives. An. Acad. Bras. Cienc. **94**: e20210825. doi:10.1590/0001-3765202220210825

Palmer Station Antarctica LTER, H. Ducklow, M. Vernet, and B. Prezelin. 2019. Dissolved inorganic nutrients including 5 macro nutrients: Silicate, phosphate, nitrate, nitrite, and ammonium from water column bottle samples collected between October and April at Palmer Station, 1991—2019. Ver 9. Environmental Data Initiative. doi:10.6073/pasta/8f9b7a10633d6eed2e8c0f2eefb8ac0c

Palmer Station Antarctica LTER, and N. Waite. 2022. Merged discrete water-column data from PAL LTER research cruises along the Western Antarctic Peninsula, from 1991 to 2020. Ver 1. Environmental Data Initiative. doi:10.6073/pasta/65c43a4688eccf8ca7cc3a2d07a0cc78

Parra, R. R. T., A. L. C. Laurido, and J. D. I. Sánchez. 2020. Hydrographic conditions during two austral summer situations (2015 and 2017) in the Gerlache and Bismarck straits, northern Antarctic Peninsula. Deep Res. I Oceanogr. Res. Pap. **161**: 103278. doi:10.1016/j.dsr.2020.103278

Plum, C., H. Hillebrand, and S. Moorthi. 2020. Krill vs salps: Dominance shift from krill to salps is associated with higher dissolved N:P ratios. Sci. Rep. **10**: 5911. doi:10.1038/s41598-020-62829-8

Prézelin, B. B., E. E. Hofmann, C. Mengelt, and J. M. Klinck. 2000. The linkage between upper circumpolar deep water (UCDW) and phytoplankton assemblages on the west Antarctic Peninsula continental shelf. J. Mar. Res. **58**: 165–202. doi:10.1357/002224000321511133

Ratnarajah, L., and A. R. Bowie. 2016. Nutrient cycling: Are Antarctic krill a previously overlooked source in the marine iron cycle? Curr. Biol. **26**: R884–R887. doi:10.1016/j.cub.2016.08.044

Saba, G. K., and others. 2014. Winter and spring controls on the summer food web of the coastal West Antarctic Peninsula. Nat. Commun. **5**: 4318. doi:10.1038/ncomms5318

Sangrà, P., and others. 2017. The Bransfield gravity current. Deep Sea Res. I Oceanogr. Res. Pap. **119**: 1–15. doi:10.1016/j.dsr.2016.11.003

Santos-andrade, M., and others. 2023. Drivers of marine CO_2-carbonate chemistry in the Northern Antarctic Peninsula. Global Biogeochem. Cycl. **37**: e2022GB007518. doi:10.1029/2022GB007518

Schlosser, P., J. L. Bullister, and R. Bayer. 1991. Studies of deep water formation and circulation in the Weddell Sea using natural and anthropogenic tracers. Mar. Chem. **35**: 97–122. doi:10.1016/S0304-4203(09)90011-1

Stammerjohn, S. E., D. G. Martinson, R. C. Smith, X. Yuan, and D. Rind. 2008. Trends in Antarctic annual sea ice retreat and advance and their relation to El Ninño-Southern Oscillation and Southern Annular Mode variability. J. Geophys. Res. **113**: C03S90. doi:10.1029/2007JC004269

Takeda, S. 1998. Influence of iron availability on nutrient consumption ratio of diatoms in oceanic waters. Nature **393**: 774–777. doi:10.1038/31674

Tovar-Sanchez, A., and others. 2007. Krill as a central node for iron cycling in the Southern Ocean. Geophys. Res. Lett. **34**: L11601. doi:10.1029/2006GL029096

Van Caspel, M., H. H. Hellmer, and M. M. Mata. 2018. On the ventilation of Bransfield Strait deep basins. Deep Sea Res. II Top. Stud. Oceanogr. **149**: 25–30. doi:10.1016/j.dsr2.2017.09.006

Venables, H. J., M. P. Meredith, and A. Brearley. 2017. Modification of deep waters in Marguerite Bay, western Antarctic Peninsula, caused by topographic overflows. Deep Res. Part II Top. Stud. Oceanogr. **139**: 9–17. doi:10.1016/j.dsr2.2016.09.005

Vera, C. S., and M. Osman. 2018. Activity of the southern annular mode during 2015–2016 El Niño event and its impact on southern hemisphere climate anomalies. Int. J. Climatol. **38**: e1288–e1295. doi:10.1002/joc.5419

Wang, B., M. Chen, F. Chen, R. Jia, X. Li, M. Zheng, and Y. Qiu. 2020. Meteoric water promotes phytoplankton carbon fixation and iron uptake off the eastern tip of the Antarctic Peninsula (eAP). Prog. Oceanogr. **185**: 102347. doi:10.1016/j.pocean.2020.102347

Wang, X., C. Moffat, M. S. Dinniman, J. M. Klinck, D. A. Sutherland, and B. Aguiar-González. 2022. Variability and dynamics of along-shore exchange on the West Antarctic Peninsula (WAP) continental shelf. J. Geophys. Res. Oceans **127**: e2021JC017645. doi:10.1029/2021JC017645

Whitehouse, M. J., A. Atkinson, and A. P. Rees. 2011. Close coupling between ammonium uptake by phytoplankton and excretion by Antarctic krill, *Euphausia superba*. Deep Sea Res. I Oceanogr. Res. Pap. **58**: 725–732. doi:10.1016/j.dsr.2011.03.006

Zhou, M., P. P. Niiler, and J. H. Hu. 2002. Surface currents in the Bransfield and Gerlache straits, Antarctica. Deep Sea Res. I Oceanogr. Res. Pap. **49**: 267–280. doi:10.1016/S0967-0637(01)00062-0

Acknowledgements

Conflict of Interest

None declared.